GOVERNMENT OF INDIA
ATOMIC ENERGY COMMISSION

SPECTROSCOPY DIVISION
ANNUAL PROGRESS REPORT FOR 1973-74

BHABHA ATOMIC RESEARCH CENTRE
BOMBAY, INDIA
1974

B.A.R.C.- 783

GOVERNMENT OF INDIA
ATOMIC ENERGY COMMISSION

B.A.R.C.- 783

SPECTROSCOPY DIVISION
ANNUAL PROGRESS REPORT FOR 1973-74

BHABHA ATOMIC RESEARCH CENTRE
BOMBAY, INDIA
1974

C O N T E N T S

BRIEF SURVEY OF R & D ACTIVITIES

A brief review of the R & D activities was presented on January 11, 1974. They are broadly -

I. ANALYSIS OF HIGH PURITY AND REACTOR GRADE MATERIALS

II. ATOMIC, MOLECULAR AND SOLID STATE SPECTROSCOPY

III. OPTICS

IV. SERVICE ELECTRONICS

The need arose for the organisation of a Spectroscopy laboratory to provide analytical service for different reactor materials. The main advantage of spectroscopy is that it requires only minute quantities of samples and enables the estimation of a large number of impurities in trace amounts simultaneously.

However, I may just mention here that the division has added x-ray fluorescence spectroscopy for analytical service during the year under review. Its potentialities are well-known and have been abundantly clear even with the few analyses carried out so far in the division. Some of these are highlighted.

It is proposed to add to the existing x-ray fluorescence spectroscopy, Auger- and photo-electron spectroscopy. Besides their application in the analysis of elements of low atomic number, from fluorine downwards, photo-electron spectroscopy is extremely useful for the studies of surface properties of solids and electronic structure studies of molecular species.

So far, infrared spectroscopy occupied a prime place in the analytical techniques. We did indeed set-up, perhaps for the first time in the country, an infrared spectrometer and used it for analysis of heavy water. With the advent of high power lasers, it is now possible to use Raman spectroscopy with equal or better ease for analytical purposes. We have recently acquired an argon ion laser with a Spex triple monochromator and a photon counting unit with other accessories. We also have been building He-Ne lasers of reasonable power.

With these, it will now be possible to study low frequency lattice vibrations and their interactions on the vibronic spectra. The laser Raman spectrophotometer will enable the identification of several impurities in micro samples (as little as 0.002 ml) and in areas as small as 10 microns. Surface impurities can be studied better by laser Raman spectroscopy.

We are aware that the rotation and vibration-rotation Raman lines are ideal for identifying minute pollutants several kilometers away. This requires an intense laser source and large light gathering and high resolution Raman spectrophotometer. With the expertise and the initial work on lasers and monochromators that we had, we shall be able to build such instruments. If one were to look for an infrared instrument, it would have to be a type Connes used for detection of CO and CO_2 in planets.

For isotopic analysis we have developed a unique method for determining the abundances of boron isotopes based on the knowledge that in a BO_2 molecule, the isotopic molecules have widely different zero-point

energies in the ground and excited electronic states. This does not, therefore, require very highly resolving instruments. This is a spin-off from molecular spectroscopy.

Basic research in spectroscopy is important, and the division undertakes research in atomic, molecular and solid state spectroscopy. Several senior scientists work on some select problems (shown under II, Atomic, Molecular and Solid State Spectroscopy) in each of the above areas with the co-operation of junior scientists. I must emphasise here that research is taken up only after discharging the analytical responsibility of the division.

Of the several areas, I shall just cite one or two research problems undertaken by us. Studies of high resolution electronic spectra give us the important data on the electronic states and the electron configurations which give rise to these states. A correct understanding of the spectra will tell us more of the molecular structure including the nuclei of atoms and a precise knowledge of the molecular parameters will help in the determination of dissociation energies, reactivities, etc.

Let us take a simple molecule like S_2. Fig.1 illustrates the importance of high resolution rotational structure studies of S_2 giving the first experimental evidence for the spin of ^{34}S to be zero. Fig.1 also shows the all important phenomenon of predissociation. In other words, if one were to irradiate a mixture of all the possible isotopic diatomic sulphur molecules with the right wavelength, it is possible to dissociate

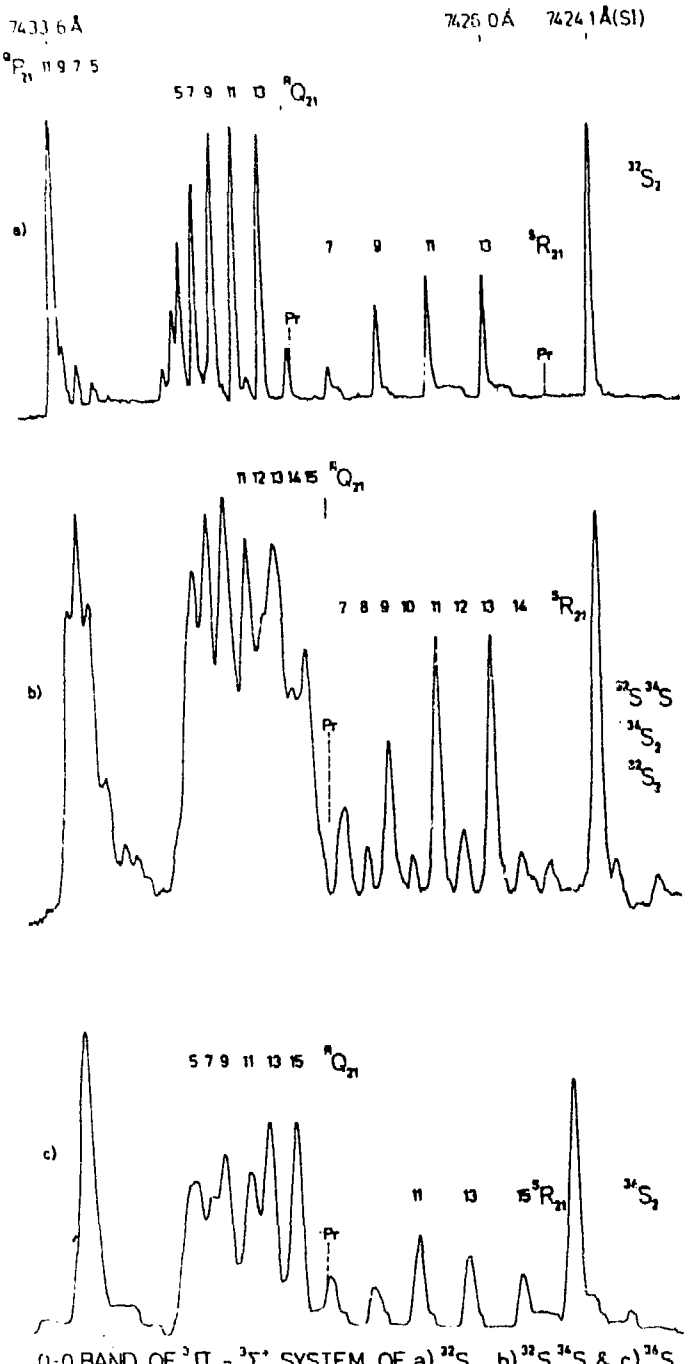

0-0 BAND OF $^{3}\Pi_{1_g} - {}^{3}\Sigma_{g}^{+}$ SYSTEM OF a) $^{32}S_2$, b) $^{32}S\,^{34}S$ & c) $^{34}S_2$

only those molecular species for which the energy matches and no other. The importance of such spectroscopic information is evident.

We are presently planning to extend such spectroscopic investigations to ^{6}Li ^{7}Li, $^{6}Li_2$ and $^{7}Li_2$ employing laser excited selective molecular fluorescence. Our own work on boron containing molecular species and NH would also be very interesting in this regard.

Suffice it to say that such research work is of fundamental importance to our own understanding and also for any technological application.

In this connection, I may mention that during the last three years, an extremely powerful means of high precision spectroscopy has emerged out of saturation techniques using lasers. Even when one is able to achieve very high resolutions with grating monochromators, Doppler broadening sets the limit to precision spectroscopy. This is got over by the novel technique of saturation or non-linear or Lamb Dip spectroscopy. This is illustrated in the studies of the ν_3 band of CH_4 known to be inactive - but made active - a prediction made in early fifties found possible after nearly twenty years.

IIT, Kanpur, is actively engaged in laser spectroscopy, though not in saturation spectroscopy. It is proposed to collaborate with them on this aspect of non-linear spectroscopy. On our part, we have so far built a 2-metre He-Ne laser with good power output. The Electronics group is working on stabilising its frequency when it can be used for saturation work.

There are other areas like plasma spectroscopy and for which spectroscopy is an ideal diagnostic tool because it is essentially an

unperturbing probe which samples a system in space and time - and we are collaborating with the Plasma Physics group in this work, and Beam Foil Spectroscopy for the study of the spectra of highly stripped atoms - we shall be making use of the facilities at Van-de-Graaf laboratory for this purpose.

Though, from the beginning it was realised that a good optics laboratory is an essential component to spectroscopy laboratory, it was started only late in 1966. For several spectroscopic investigations, it is necessary to have instruments using optics of high quality and precision. The spectroscopy laboratory has, therefore, undertaken the preparation of high quality and precision optics like Fabry-Perot plates, lens systems, large spherical surfaces etc. with which high resolution interferometers and spectrographs of large light gathering power can be built - and are actually built as described later.

Interferometry is one of the major research areas in optics and the scientist in-charge, Dr. M.V.R.K. Murty, is well-known for his work in this field. We also have a younger scientist trained on thin films at the Imperial College of Science and Technology who has been working on the project, interference and band-pass filters.

In the R & D Profile, certain specific projects are identified and are proposed in collaboration with Technical Physics Division. These include spectrophotometers, monochromators, etc. Fabrication of such instruments will bring out the best of technical competence available in B.A.R.C.

It has been a cursory glance, but still, I hope, it gives a feeling of the amount of effort involved. As mentioned earlier, the first priority has always been to analytical service. Over the years, there has been an increasing demand for analytical services from various divisions of B.A.R.C and other units of DAE - not to mention outside institutions.

- N.A. Narasimham

I. ANALYSIS OF HIGH PURITY AND REACTOR GRADE MATERIALS

I(a) EMISSION SPECTROSCOPY

1. Spectrographic Determination of Boron in Uranium and its Oxides

(S.V. Gramporohit and V.S. Dixit)

Boron has a large absorption cross-section for thermal neutrates and hence it is necessary to detect it at very low levels in nuclear grade uranium. Further, during the processing of uranium, it is likely to be contaminated with boron and hence it is important to determine boron at various stages of fabrication of uranium. Among the methods tried, there are a number of single and mixed spectroscopic carriers for boron analysis. A mixture of silver chloride and strontium fluoride in the ratio 4:1 was found to be a suitable carrier with which the sensitivity was improved appreciably. A method was, therefore, developed using this carrier for B-analysis. In this method, the spectra are excited using a d.c. arc and recorded on SA-1 emulsion using Hilger large quartz spectrograph. The background was found to be quite low and it has been possible to use multiple exposures for analysis of one sample. With these modifications, it has been possible to attain a detection limit of 0.01 ppm for boron - a sensitivity of an order of magnitude greater than the previous methods. The reproducibility and accuracy of the method has been checked and is found to be satisfactory.

2. Direct Spectrographic Determination of Boron in UF_4

(P.S. Murty, S.M. Marathe and P. Rugmini Bai)

The standardisation of a method for the direct determination of boron in UF_4 has been completed. UF_4 sample is mixed with sodium fluoride

in the ratio 20:1 by weight and two hundred milligrams of the mixture is loaded in a carrier-distillation electrode (U.C.C. type 1998). It is excited at 5 amp. d.c. for 6 seconds and spectra are photographed on a Hilger large quartz spectrograph. Antimony is used as the internal standard element. Using the line pair B 2497.7 Å/Sb 2445.5 Å boron is estimated with a sensitivity of 0.07 ppm. The precision of estimation is ± 16%.

3. Spectrographic Analysis of Semiconductor Grade B_2O_3

(R.V. Subramanian, R.M. Dixit and T.R. Saranathan)

An emission spectrographic method for the estimation of trace amounts of Al, Ca, Cr, Fe, Mg, Mn, Ni, Pb, Si and Sn in high purity boron trioxide has been developed. The sample after conversion to boric acid is mixed with a carrier consisting of sodium fluoride and graphite in the ratio 1:4. By use of this carrier, the background due to BO emission is reduced. The detection limits lie in the range of 2-12 ppm for different elements. The precision of the method ranges from 7-18% for these elements while the relative error is ± 15%.

4. Spectrographic Analysis of High Purity Aluminium Metal

(L.C. Chandola and I.J. Machado)

Aluminium metal standards are available commercially but these contain few impurity or alloying elements like Cu, Fe, Mn, Si, Ti and Zn. For the aluminium used in reactors many more impurities like B and Cd have also to be looked for. The analysis has, therefore, to be done

indirectly by converting the metal to oxide and analysing by comparison with synthetic standards. Pure aluminium oxide is available commercially for the preparation of standards. The problem was to prepare aluminium oxide from the metal and to know whether the impurities are retained or lost during the conversion process.

A method was developed to convert the aluminium metal to aluminium oxide for this analysis. For this, the metal is dissolved in hydrochloric acid, the Al is precipitated with ammonium hydroxide, and the supernatant solution and precipitate are evaporated on a water bath. The dried hydroxide is then ignited to aluminium oxide. The aluminium oxide so obtained is analysed by the method developed earlier[1].

To find out whether the impurities are retained or lost during the conversion to oxide, an aluminium standard from AA series supplied by Johnson Matthey & Co. was converted to oxide by the method described above. It was found that impurities like Cu, Fe, Mn and Ti were retained but impurities like Si, which have volatile chlorides, are partially lost during the process.

The overall standard deviation for determination on aluminium oxide was found to be $\pm$ 11%.

---

1. L.C. Chandola and I.J. Machado, Spectroscopy Division, Annual Progress Report 1972-73, BARC-684, 16 (1973).

5. Spectrographic Analysis of High Purity MnO_2

(V.A. Job, S.B. Kartha, G. Krishnamurty and Sheila Gopal)

Emission spectrography provides a rapid method for the simultaneous estimation of various impurities present in manganese dioxide which is used as a depolarizer in dry cells. These impurities act as poisoners to the battery system and therefore have to be analysed in trace amount.

We have developed a d.c. arc emission method for the quantitative estimation of 20 impurity elements using preheated manganese dioxide. The aim was to attain lowest possible estimation limits for as many impurity elements as possible. Several buffer combinations have been tried. It was found that low detection limits cannot be attained simultaneously for all the impurity elements with any of the buffers we have studied. Therefore, two separate methods were developed. In one method, 5% BaF_2 is used as buffer to get good sensitivity for the elements such as As, B, Sn, Cd etc. For the elements like V, Ti, Cr and Fe, the sample is mixed with an equal weight of graphite. Ga and Mn lines are used as internal standards.

A set of standards containing the impurity elements in the concentration range of 500 - 1 ppm were prepared and mixed with the buffers in the required ratio. 30 mgs of this mixture loaded in the $\frac{1}{4}$" U.C.C. graphite electrode drilled to the required depth is excited in a d.c. arc at 10 amp. current for 20 seconds. The spectra are recorded on a 3.4 meter JACO grating spectrograph with 30,000 l.p.i. grating blazed

at 3300 Å. The estimation range for various elements are given below.

Sn,Bi,Ag,Pb,Sb,In	..	2 - 100 ppm
As,Co,B,Mo,Cd,V,Cu,Na,Zn,Ni	..	10 - 100 "
Cr,Ti,Fe ..	..	20 - 500 "

The method is found to be reproducible within ± 10% for most of the elements. Recovery tests showed that preheating the sample did not result in the loss of any of the impurity elements.

6. Spectrographic Analysis of Wear Metals in Lubricating Oils

(S.V. Grampurohit and P. Meenakshi Raja Rao)

An emission spectrographic method for the determination of wear metals Si, Fe, Mg, Ni, Al, Ti, Cu, Zn, Ag, Mo, Pb, Cr and Sn in aviation oils is being developed. The method consists of two parts: one for the analysis of all elements except silicon and magnesium and the second for the analysis of Si and Mg.

Part 1 - Since aviation oils are practically ashless, conventional ashing techniques are not applicable. In the present method, therefore, 1 gm of oil is ashed on 100 mg of gallium oxide which contains 10% of lithium fluoride as carrier. Standards are prepared on gallium oxide base for concentration range of 5 ppm to 100 ppm which also contain 10% LiF as carrier. The spectra were recorded at 10 amps d.c. on a large quartz spectrograph in the region 2400-3450 Å. Recovery tests showed that recovery for Si and Mg was poor. So a separate method is being

developed for the determination of Si and Mg.

Part 2 - Various matrices were tried for the analysis of Si and Mg in oils and lanthanum oxide with a 10% NaF-calcium carbonate as carrier internal standard mixture (9:1) was found most suitable. Samples are ashed on lanthanum oxide base to which the NaF-calcium carbonate mixture was added. Carrier mixed standards ranging from 5 ppm to 100 ppm were also prepared. To avoid the possibility of silicon contamination samples and the standards were ground in boron carbide mortar. The spectra were recorded at 12 amps. d.c. in a large quartz spectrograph in the region 2400-3450 Å. Recovery tests showed that Si and Mg are completely recovered in this case. By this method, most of the other elements of interest also were recovered well but in lanthanum oxide matrix Al and Cr do not get excited with good enough intensity. So the analysis has to be carried out in two steps.

By adopting these methods the lowest detection limit that could be achieved was 1 ppm on sample basis, with 1 gm of sample being ashed. It is obvious that by increasing the amount of sample taken for ashing, sensitivity could be increased.

7. Spectrographic Analysis of Thallous Iodide

(P.S. Murty and P. Rugmini Bai)

A semiquantitative spectrographic method has been developed for the analysis of thallous iodide. The sample is mixed with pure graphite powder in the ratio 1:1 by weight and fifteen milligrams of the mixture

is arced at 10 amp. d.c. The spectra are recorded on a Hilger large quarts spectrograph in the region 2400-3350 Å. Trace impurities like Pb, Co, Ca etc. are determined with a sensitivity ranging from 5 to 25 ppm.

8. Spectrochemical Analysis of Phosphorus Compounds

(T.R. Saranathan, M.J. Kamat and T.S. Sugandhi)

In an effort to make the existing semiquantitative method[1] for the determination of impurities in PCl_3 and $POCl_3$ quantitative, it was necessary to ensure easy removal of the sample after preconcentration. Also, due to the formation of phosphoric acid in the samples it was difficult to evaporate the sample completely on graphite. Hence it was necessary to convert the final evaporated sample into a phosphate. Of the two phosphates of Ca and Bi, the latter was preferred due to its denseness. After experimenting with LiF, NaF and graphite as carriers and buffers to be mixed with the phosphate, a mixture of LiF and graphite was found to be most suitable. Standards of bismuth phosphate for 15 impurities were prepared. Their spectra were recorded on Hilger large quarts spectrograph with d.c. arc excitation and the working curves have been drawn. Final recovery experiments for samples are being carried out.

---

1. M.J. Kamat, T.R. Saranathan and T.S. Sugandhi, Spectroscopy Division Annual Progress Report, 1972-73, BARC-684, 12 (1973).

9. Determination of Boron in Calcium Fluoride Using a Carrier Distillation Technique

(S.V. Grampurohit and V.S. Dixit)

Calcium fluoride is used extensively as lining material in the reduction of uranium tetrafluoride to uranium metal. It is necessary, therefore, to analyse calcium fluoride for impurities like boron which possess high capture cross-sections for thermal neutrons.

A carrier-distillation method is described here for the estimation of boron in calcium fluoride. The sample is mixed with 5% copper oxyfluoride containing 500 ppm of gallium. Copper-oxyfluoride acts as carrier and gallium as internal standard. 50 mg of this mixture is loaded in pre-arced U.C.C. 1990 electrode and excited using 15 amp. d.c. arc. The spectra are recorded in the region 2200-2850 Å on SA-1 emulsion using a Hilger large quartz spectrograph. The sensitive line of boron at 2497.7 Å is used and a detection limit of 0.1 ppm is attained. The precision of the method is $\pm$ 12%.

10. Analysis of Trace Impurities in Strontium Carbonate by Spectrographic Technique

(B.R. Vengsarkar and M.D. Saksena)

In electronic industry, strontium carbonate is required in a highly purified form for cathode spraying and thus it becomes necessary to develop an analytical method for the analysis of $SrCO_3$ for trace impurities. A spectrographic method is, therefore, being developed for

the analysis of 11 impurities.

Initial experiments with direct arcing of $SrCO_3$ showed that burning of $SrCO_3$ was erratic and after a few seconds the bulk of the charge used to come into the arc. The volatilization studies also showed that the impurities like Fe, Al, Cu, Si, Mg take a prolonged time for excitation because of the low boiling point of $SrCO_3$. In order to improve the volatilization and to have smooth burning, experiments were conducted by mixing different ratios of matrix with graphite as a buffer. It was experimentally found that mixing in equal proportions of $SrCO_3$ and graphite was most suitable in increasing the sensitivity. Volatilization rates of different impurity elements were also studied to determine the time of exposure.

A set of standards containing the impurity elements in two groups were prepared in the concentration ranges of 1 to 20 ppm and 10 to 200 ppm and were then mixed with graphite in equal proportions. 50 mg of charge is excited in a d.c. arc at 15 amp. current for a period of 30 seconds on JACO 3.4 metre grating spectrograph equipped with 30,000 l.p.i. grating blazed at 3300 Å. The following are the ranges of estimation for various elements:

Al, Cu, Fe, Mg, Pb, Si	..	1 to 20 ppm
Cd	.. ..	10 to 200 ppm
Zn, Na, Ba, Ca	..	50 to 500 ppm

Chromium and bismuth are used as internal standard elements.

Since the elements like Na, Ca and Ba are having sensitive lines in the region 4000 - 6000 Å experiments are conducted on Hilger's large glass and quartz spectrograph to get higher sensitivity for these elements. Further experiments are in progress to determine the precision and sensitivity of the method.

11. Spectrographic Analysis of High Purity Europium Oxide

(P.S. Murty and S.M. Marathe)

A spectrographic method has been developed for the estimation of Nd and Dy in high purity europium oxide. In order to make use of the sensitive lines of Nd and Dy, most of which lie in the CN band region, the excitation of Eu_2O_3 has been done in an oxygen atmosphere using a Stallwood jet assembly. The spectra are recorded on Ebert 3.4 metre plane grating spectrograph in the second order using a 30,000 l.p.i. grating. The grating is blazed at 7,500 Å in the first order. Using Nd 4061 Å and Dy 4078 Å the detection limit obtained for these elements is 0.005%.

12. Spectrographic Determination of Trace Elements in Basalt Rocks

(L.C. Chandola)

Basalts are the main volcanic rocks in the Deccan Traps in Maharashtra. In order to find the history of association of this host rock with various mineral pockets, it is necessary to do the trace element analysis of this rock. The main problem associated with spectro-

graphic analysis of rocks for trace elements is the non-availability of standards. It was found from literature that average basalt composition was as follows:

SiO_2	- 50%	Fe_2O_3	- 10%
Al_2O_3	- 15%	CaO	- 10%
MgO	- 10%	TiO_2	- 2%
Na_2O	- 3%		

Standards were, therefore, prepared on the matrix described above. 49 elements contained in Spex Mix were added to the matrix at various concentrations. These standards and samples were then mixed with pure graphite and pure zinc oxide in the ratio 1:1:1. One weak zinc line was used as internal standard. The samples and standards were excited in a d.c. arc run at 10 amp. current and the spectrum was photographed in two regions on large quartz spectrograph. Analysis of about 25 elements could be done by this technique. Of these B, Be, Co, Cr, Li, Mn, Ni, Sr and V were found to be present in trace levels and were quantitatively estimated.

13. Determination of Iron in Di-Ammonium Hydrogen Phosphate

(S.V. Grampurohit and V.N.P. Kaimal)

Direct spectrographic estimation of iron in purified di-ammonium hydrogen phosphate cold not be carried out as the material had a tendency to be ejected from the electrode. In addition, ammonium compound itself prevented the impurity spectrum from being suitably excited. On the other hand, because of the presence of phosphate radical, atomic absorption

method could not be employed. Hence a spectrochemical method based on t... extraction of iron using solvent extraction technique followed by s. trographic analysis has been worked out for this determination.

One gram of di-ammonium hydrogen phosphate is dissolved in triply distilled water and the pH of the solution adjusted to 10 using 25% ammonia. A known volume of 2.5% oxine is added dropwise to the above solution and shaken slowly. Iron forms a complex with oxine and is extracted using chloroform. The separated organic layer is collected and the aqueous layer is shaken again with another 10 ml of chloroform. The organic layers are collected and evaporated over 200 mg of graphite and mixed in an agate mortar.

15 mg of this mixture is loaded in pre-arced graphite electrode ($\frac{1}{4}$" U.C.C) and excited using a d.c. arc at 10 amps. The spectra are recorded on SA-1 emulsion in the region 2400 to 3300 Å with the help of Hilger large quartz spectrograph. The iron line at 2598 Å is chosen as the analytical line. It has been possible to estimate iron upto 1 ppm level.

14. Spectrochemical Analysis of Noble Metal Alloys

(L.C. Chandola and V. Mahajan)

Noble metal alloys are used in the tips of fountain pen nibs. A method was developed for the analysis of these pen tips. The tips were dissolved in aqua regia + hydrofluoric acid and the solution was dried on graphite. Suitable dilutions in graphite were prepared.

Quantitative estimations were made by comparing the spectra from these dilutions with two sets of graphite base standards. One set of standards contained 49 common impurities and the other set 10 noble metals. Analysis by the above methods showed that the pen tips consist of Ru-Ni-Co alloy.

15. MISER - Micro Spectral Emission Analyser

(S.L.N.G. Krishnamachari and B.R. Vengsarkar)

In order to check the efficiency of Micro Surface Emission Analyser[1], the spectra of copper-chromium alloy samples have been studied for uniformity of distribution of chromium in the samples. The spectra were recorded on Hilger's Baby Quarts Spectrograph with an exposure of 2 minutes. A set of preliminary experiments showed that the sensitive lines of chromium are easily excited with copper as counter electrode instead of tungsten and the latter exhibited a more complex spectrum.

Since an exposure of 2 minutes leads to a considerable large crater on the sample, it is decided to reduce the time of exposure by using a spectrograph of large aperture and medium resolution. For this purpose, a quarter-meter grating monochromator fabricated in the division is being converted into a spectrograph by incorporating a camera attachment to record the spectra.

---

1. S.L.N.G. Krishnamachari and B.R. Vengsarkar, Spectroscopy Division Annual Progress Report for 1972-73, BARC-684, 28, (1973).

16. A Modified Method for Analysis of Rare Earths in High Purity Gadolinium Oxide

(S.V. Grampurohit and V.N.P. Kaimal)

Spectrographic methods are widely used for the analysis of rare earths in high purity rare earth oxides. As the spectra of rare earth elements are highly complex, one has to use high dispersion spectrographs to carry out the analysis. Another difficulty that is encountered is that the sensitive lines of many rare earth elements lie in the cyanogen region and hence could not be used. To overcome these difficulties, a spectrographic method is worked out to determine trace rare earth impurities in high purity gadolinium oxide. A Jarrell Ash 3.4 meter grating spectrograph having a 1200 grooves/mm grating is used in the second order at a reciprocal linear dispersion of 1.2 Å/mm. A stallwood jet is used with oxygen flowing at a rate of 15 litre/minute. This helped in suppressing the cyanogen bands and with these changes it has been possible to attain a detection limit of 0.0025% for Sm, Dy and Y. The recovery of the method was compared with X-ray fluorescence analysis and is found to be quite satisfactory.

17. Spectrographic Determination of Trace Elements in Zeolites

(L.C. Chandola)

Zeolite mineral pockets are found in abundance in basalt rocks around Poona in Maharashtra. In order to find the history of origin of this guest mineral in the host rock, basalts, it is necessary to do the

trace element analysis. The standards for these minerals are not available and, therefore, were prepared in the laboratory. The following average composition of the zeolites was taken as the matrix:

SiO_2	..	60%
$CaCO_3$	..	10%
KCl	..	1.5%
Al_2O_3	..	25%
Na_2CO_3	..	3.5%

To the above matrix, the Spex Mix powder containing 49 elements was added at various concentrations ranging from 10 ppm to 1,000 ppm. These samples and standards were then mixed with graphite and zinc oxide in the ratio 1:1:1. The spectrum was obtained in a manner similar to basalts[1]. In all, 25 elements were looked for and out of these, Ba, Cu, Fe, Li, Mg, Ni, Sr and V were found to be present in trace levels. These were quantitatively estimated.

1. L.C. Chandola, page 10 of this Report.

18. Spectrographic Determination of Trace Metals Collected on Air Filters

(G. Krishnamurty, M. Saraswathy and O. Thomas)

Environmental air sample analysis has gained importance in the recent times in view of atmospheric pollution, especially in the industrial and urban areas. The pollutants have acute physiological effects

on human health. The particulates in the polluted community environment .sists of a wide range of metallic elements besides a variety of anic matter[1].

As part of the programme of the environmental sample analysis, we have developed an emission spectrographic method for the quantitative estimation of trace metals Mn, Pb, Cr, Ni, V, Cd, As and Zn in atmospheric particulates.

In this method, air is aspirated through a Whatman No.41 filter paper by means of the suction head of a high volume air sampler for two hours. In order to avoid the losses of the trace metals in the sample, we have adopted the wet ashing method. The sample collected on the filter paper is charred with 1 ml of sulphuric acid (G.R. grade) to decompose the organic matter of the filter paper. 5 ml of concentrated nitric acid (doubly distilled) is added dropwise with subsequent stirring. The clear solution left behind is then evaporated slowly to dryness on a hot plate at about 250°C.

The weight of the residue left after charring usually varies between 30 mg to 50 mg. This is made upto 75 mg by adding pure conducting graphite (UCC, 200 mesh). 25 mg of pure graphite containing 0.2% of Ge_2O_3 which acts as the internal standard is mixed with this and ground thoroughly.

25 mg of the charge is loaded in $\frac{1}{4}$" U.C.C. graphite electrode (anode) and is excited in 10 amp. d.c. arc for 30 seconds. Spectra are recorded on a large quarts prism spectrograph in the wavelength region 2500-3500 Å.

The concentration ranges of the various impurities are given below:

Mn, Pb, Cr, Ni, V	..	1 - 100 ppm
Cd	..	10 - 500 ppm
As, Zn	..	50 - 1000 ppm

The average standard deviation of most of the elements is about 11%.

Detailed examination of the spectra of samples collected over filter papers have shown that certain elements like Mg, Si, Al, Cu, Ca and Fe, if present at 0.2% or above, will suppress the intensities of trace elements and hence the results may not be quantitative for such samples.

1. Jae Young Hwang, Anal.Chem. 44, 20A, (1972).

19. A Spectrographic Method for the Analysis of Soil Samples

(V.P. Bellary, V.B. Kartha and Y.A. Sarma)

The analysis of trace elements in soil samples is of importance for pollution studies as well as other purposes.

A d.c. arc spectrographic method for the analysis of trace elements in soil samples is being developed for this purpose. Most of the organic constituents of the sample is destroyed by dry ashing at 450°C in a furnace. This dry ashed sample is mixed with 33% graphite and 6% Sb_2O_3 containing internal standard Pd at 0.02%. The sample and synthetic standards are excited in a d.c. arc at 15 amps. in an atmosphere of oxygen. The spectra

were recorded on an Ebert 3.4 meter grating spectrograph with 30,000 l.p.i grating blazed at 3300 Å, in the first order. At present, the effect of major components of soil like Si, Al, Fe, Ca, Na and K on the common trace elements is being studied. The following Table gives the range of analysis and other details for some of these trace elements.

Sr.No.	Elements and the special line used in the present work in Å.	Average amount in soil in ppm.	Present range of determination in ppm
1.	Cr 4254.3	8 - 1000	5 - 1000
2.	Ni 3493.0	7 - 700	5 - 1000
3.	Mn 4030.8	200 - 6000	10 - 1000
4.	Pb 3639.6	2 - 120	5 - 500
5.	V 3185.4	20 - 800	5 - 1000
6.	Zn 3345.0	10 - 350	5 - 500
7.	Ag 3280.7	0 - 1	0.1 - 10
8.	Cu 3247.5	2 - 100	1 - 500

20. Spectrographic Analysis of Trace Elements in Food Materials

(M.N. Dixit, G.L. Bhale and Annamma Joseph)

The analysis of trace elements in food materials is important for biological as well as environmental pollution studies. A spectrographic method was, therefore, developed for the analysis of food materials, mainly wheat flour and potatoes for trace elements.

The food material is ashed in a muffle furnace at 550°C, and the ash is mixed with pure graphite in the ratio 1:2. 20 mgms of the mixture is arced at 10 amps. d.c. and the spectra are recorded in the region 2700 - 3300 Å on a 3.4 meter Jarrel Ash spectrograph at a dispersion of 2.5 Å/mm.

Standards were prepared by mixing together a synthetic matrix and the graphite based spex standards in the ratio 1:2.

The elements As, Cd, Cr, Fe, Mn, Ni, Pb, V and Zn can be estimated in the range of 5 to 50 ppm with an average standard deviation of ± 15%.

I(b) X-RAY FLUORESCENCE ANALYSIS

1. A Systematic Study of the Effect of Various Experimental Parameters on the X-ray Fluorescence Determination of HfO_2 in High Purity ZrO_2.

(Jura Mohammad Qurbani*, P.P. Khanna, and R.M. Agrawal)

The XRF determination of traces of HfO_2 in high purity ZrO_2 pose difficulty in the selection of experimental parameters and analytical lines for Hf owing to the almost complete overlap of the second order of ZrK_α line with first order HfL_{α_1} line and substantial overlap of the second order ZrK_{β_4} with the first order $HfL_{\beta_{1,6}}$ line. A systematic study of the effects of the various available experimental parameters on the determination of traces of HfO_2 in zirconia was, therefore, undertaken.

The Philips semiautomatic X-ray spectrometer PW 1220 with associated equipment has been used in these studies. A master standard of 2% HfO_2 in ZrO_2 has been prepared by dry-mixing calculated amount of HfO_2 in the highest available purity zirconia. This has been diluted by requisite proportion of zirconia to give the standards in the range of 50 ppm to 1% HfO_2 in ZrO_2. These standards are mixed with equal proportion of boric acid as a binding material and briquetted to standard 1½" dia. double layer pellets using boric acid as the backing pellet material. These pellets have been used to study the effects of the following experimental parameters on the lowest detection limits, sensitivity and precision of the results:-

---

* On deputation from Faculty of Science, University of Kabul, Kabul, Afghanistan.

i) Tube voltage and current;

ii) Collimators (Coarse and Fine);

iii) Scintillation and flow proportional counters;

iv) Choice of analytical lines HfL_{α_1}, $HfL_{\beta_{1,6}}$ and HfL_{β_2}

LiF(200) analysing crystal and pulse height discrimination has been used in all the cases.

From these studies the optimum experimental parameters to give the highest sensitivity and the lowest detection limit have been obtained. The limits of detection obtained was 150 ppm, which includes 100 ppm due to residual HfO_2 present in the highest purity ZrO_2 used for the preparation of standards. This residual HfO_2 content in ZrO_2 used, has been determined by XRF only during the course of these studies. Thus better detection limit could not be obtained owing to the limitation of the purity of the zirconia available.

The precision of the method varies with the range of HfO_2 content and a typical value is $\pm$ 5% for the range 0.05% - 0.1%.

2. An X-ray Fluorescence Method for Analysis of Zn, Zr and U in ThO_2

(R.M. Dixit and S.K. Kapoor)

An XRF method for the determination of Zn, Zr and U in thoria has been developed. Thoria sample is mixed with 10% boric acid as binder and this mixture is pressed into a double layer pellet. Tungsten target tube with power of 60 KV - 35 mA is used for exciting ZnK_α, while

for ZrK_α and UL_α a power of 85 KV - 25 mA is used. The estimation limits of Zn, U and Zr are 10, 50 and 100 ppm respectively. The interference between the L_{α_2} and ZrK_α is studied and ZrK_α in second order of LiF(200) crystal is used for analysis. The lower estimation limit for U and Zr is likely to be improved by use of LiF(220) crystal.

The average precision of the method is about $\pm$ 12%.

3. Analysis of Individual Rare Earths in Rare Earth Mixtures

(R.M. Agrawal, P.P. Khanna and S.K. Malhotra)

Two of the XRF methods for the determination of individual rare-earths in rare-earth mixtures are i) inert dilution with calcium as oxalate[1] and, ii) solution dilution method of Rose et al[2]. We have compared these two methods to assess their relative merits. The two approaches are found to give results in good agreement, the precisions and accuracies obtained being equally good. However, the solution dilution method can be used with a small quantity (a few mg) of the sample, whereas the inert dilution by calcium requires relatively larger amount (a few hundred mg) of the sample. As regards sensitivity also, the solution-dilution method has been found to be superior compared to the other.

1) Locally developed for ease and rapidity

2) Harry J. Rose et al, Advan. in X-ray Anal. 11, p.34-36 (Plenum Press 196

4. X-ray Excited Optical Fluorescence of Rare Earths in Minerals

(T.R. Seranathan, M.J. Kamat and T.S. Sugandhi)

Studies on the XEOF spectra of rare earths in minerals are being continued. Preliminary experiments on three minerals - monazite, pyrochlore and uranamite - show luminescence only when they are incorporated in a suitable host after dilution with pure U_3O_8. The spectra with four dilutions 1:50, 1:20, 1:10 and 1:5 were recorded by exciting the quarternery oxide $2Li_2O.SrO.UO_2.2WO_3$ with X-rays.

In the case of monazite, the fluorescence intensity increases with dilution whereas for pyrochlore it decreases. This is probably due to the elimination of matrix effect by dilution in the former and reduction of the actual rare earth concentration with dilution in the latter mineral. In uranamite, the intensity of the lines of Gd and Dy increase with dilution while for Sm and Pr it decreases. A detailed study of the intensity pattern is in progress.

5. An XRF Method for Analysis of Sm, Eu, Gd, Dy, Ho and Y in Tb_4O_7

(L.C. Chandola, I.J. Machado and A.M. Mohile)

An XRF method has been developed for the determination of Sm, Eu, Gd, Dy, Ho and Y in terbium oxide using the Philips model PW 1220 spectrometer. The range of determination is 0.01% to 1%. The terbium oxide is converted to terbium oxalate and mixed with an equal amount by weight of boric acid as binder. A double layer pellet of boric acid and sample + boric acid is made. It was possible to use $L_{\alpha 1}$ lines for all the rare-

earths determined. For Y the K_{α} line was used. LiF crystal in the f... order was employed for dispersion. Flow proportional counter was u for rare earths and scintillation counter for yttrium. An interference to Dy L_{α_1} line at $2\theta = 56.58$ was suspected from Eu L_{β_1} line at $2\theta = 56.94$. E eriments were done with synthetic samples having known amounts of Dy and Eu and no noticeable interference was observed. The precision of the method is $\pm$ 5%.

6. Determination of Nb, Ta and Ti in Ore Concentrates

(R.M. Agrawal, P.P. Khanna and S.K Malhotra)

The direct XRF method[1] for the determination of tantalum in neobate/tantalate mineral concentrates has been modified in order to increase the precision and accuracy of the method and also to extend the method for determination of Nb and Ti. The method consists in fusing the sample with potassium bi-sulphate followed by dissolution and subsequant incorporation on an inert matrix. The resulting product is then analysed by XRF using standard procedure. The chemical treatment and dissolution eliminate the heterogeneity and particle size effects resulting in better precision and accuracy.

(1) Spectroscopy Division, Annual Progress Report for 1972-73, BARC-684, (1973), pp.39-40.

7. Determination of Thorium in Uranium by XRF Method

(R.M. Dixit and S.K. Kapoor)

Preliminary studies on XRF determination of Th in uranium in the range of 50 to 1000 ppm have been completed. Th L_{α_1} line can be easily

resolved from U L_{α_1} line in first order of LiF(200) crystal, using coarse (480 u) collimation. The lower estimation limit of thorium in uranium in preliminary studies is found to be 50 ppm, which can be improved further by refinements in experimental conditions. Th L_{α_1} line is excited by tungsten target X-ray tube working at 85 KV - 25 mA.

8. Intensity Studies on XEOF of Rare Earths in Thorium

(T.R. Saranathan, M.J. Kamat and T.S. Sugandhi)

While applying the XEOF technique for the analysis of rare earths in thorium nitrate samples containing Si 200 ppm it was necessary to remove it with HF treatment. It was observed that the addition of HF increased the intensity of the lines of Gd, Sm, Dy, Eu and Pr by a factor of 5 to 20. Apart from this the intense wide band emission of ThO_2 at 4050 Å is suppressed completely with HF treatment. Figs. 1 and 2 indicate these observations. This will be useful in analysing comparatively impure samples diluted with pure nitrate and still retain the required sensitivity.

In the case of HCl and HBr additions, there is no change in intensity upto a certain stage (0.1 ml and 0.2 ml of conc. HCl and HBr respectively in 2 gms of ThO_2) after which there is considerable suppression of intensities in the case of HCl only.

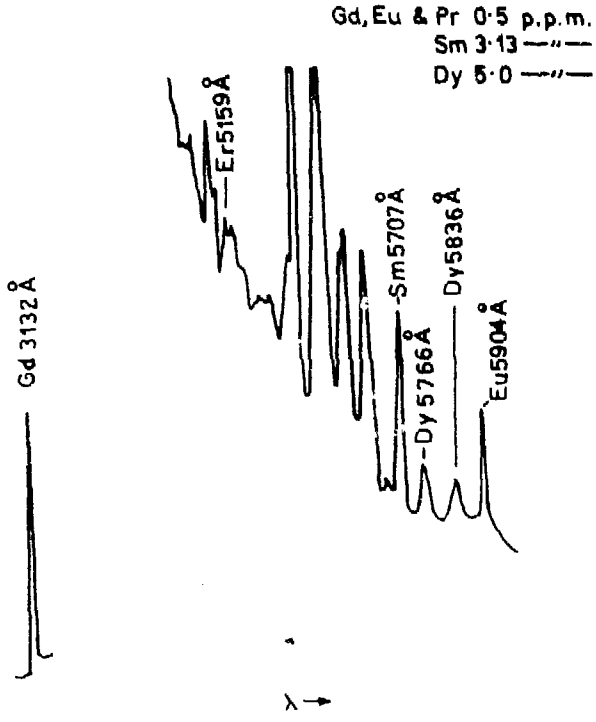

FIG. 1. X.E.O.F. OF R.E.E. IN ThO_2 WITHOUT HF TREATMENT.

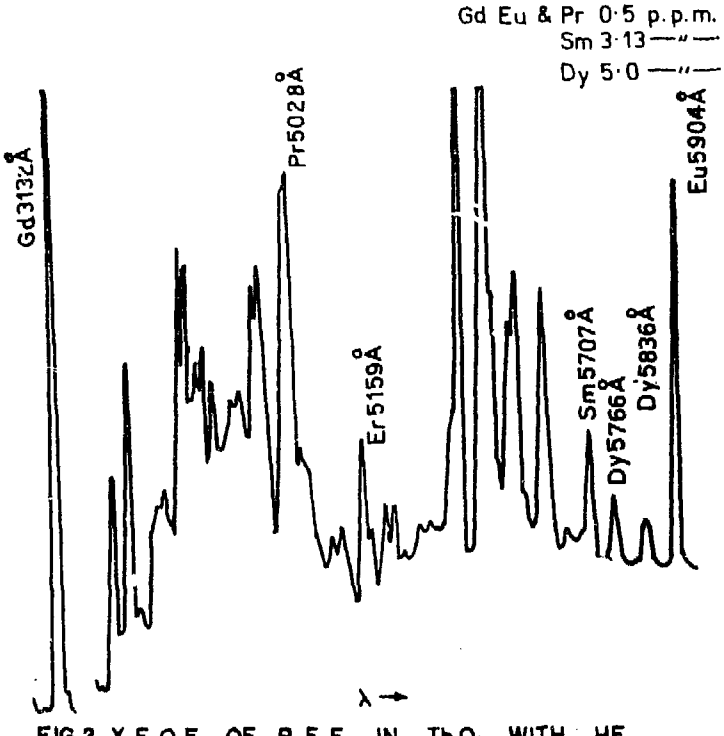

FIG. 2. X.E.O.F. OF R.E.E. IN ThO_2 WITH HF TREATMENT.

9. XRF Determination of Individual Alkaline Earth Elements in Double and Triple Alkaline Earth Carbonates

(R.M. Agrawal and P.P. Khanna)

XRF methods have been developed for the analysis of double and triple carbonates of alkaline earths for individual alkaline earth elements. During the course of analysis of triple carbonates, it was observed that the geometrical method of matrix effect correction by concentration triangle technique of Taylor et al[1] is not applicable in such systems. The method and the approach has been modified, so that they work reasonably well with such a ternary system.

A systematic study of the merits and limitations of the modified approach to various other ternary and pseudo ternary systems is in progress.

1. Taylor et al, Anal.Chem. 33, 1699-1706 (1961)

10. Determination of Dopant Cerium in Thermoluminiscent Calcium Sulphate

(R.M. Agrawal and P.P. Khanna)

Using the procedure similar to the determination of Dy and Tm in $CaSO_4$ reported earlier[1], an XRF method has been developed for the determination of cerium in thermoluminiscent grade $CaSO_4$ (Ce) in the concentration range .005% - 2%.

1. BARC Report No.BARC-684 (1973), p.43.

11. Analysis of As and Zn in High Purity Tin Oxide by an XRF Method

(R.M. Dixit and S.K. Kapoor)

As and Zn in high purity tin oxide have been determined in the range of 10 - 1000 ppm by an XRF method.

Tin oxide sample is pressed in the form of a double layer pellet with 50% boric acid as a binder. 500 mg of tin oxide was found adequate to give adequate thickness and optimum peak to background ratio.

Both As and Zn can be estimated upto 10 ppm in Pb free tin oxide. The average precision and accuracy of the method is within ± 15%.

A correction procedure for determining arsenic in tin oxide even in the presence of 200 - 500 ppm of Pb has also been worked out.

12. Direct XRF Determination of Individual Rare Earths in ThO_2

(R.M. Agrawal and P.P. Khanna)

The XRF method for the determination of individual rare-earths in U_3O_8 reported earlier[1] has been extended for the determination of trace rare-earths in ThO_2 also. Range of determination is .005% - 1%.

---

1. BARC Report No. BARC-684 (1973), p.43.

13. XRF Determination of the Platinum Content of Chloroplatinic Acid Solution

(R.M. Agrawal and S.K. Malhotra)

Accurate determination of platinum content of chloroplatinic acid solution is required in order to assess the suitability of the latter in the electroplating baths and also for evaluating the cost. Small amount of the solution could only usually be spared for such analyses. Standard solution-dilution method of Rose et al[1] has been modified and used for this analysis using standard platinum solutions for addition and standardisation.

1. Harry J. Rose et al., Advan. in X-Ray Anal. 11, p.25, (Plenum Press, 1968).

14. Analysis of Gases by XEOF

(T.R. Saranathan, M.J. Kamat and T.S. Sugandhi)

Work on the XEOF study of traces of nitrogen in argon has been initiated. A glass chamber has been fabricated with mylar or aluminium window for X-ray excitation and quartz window for the study of the resulting optical fluorescence. Further improvements are planned with the experience acquired so far with this chamber.

I(c) INFRARED AND RAMAN SPECTROSCOPY

1. Determination of Water in Organic Solvents by Infrared Spectrophotometry.

(Y.A. Sarma and V.B. Kartha)

The presence of water and its influence on the properties and reaction of organic compounds makes its quantitative determination necessary to the analyst. Of specific analytical importance is the need to determine the water content of organic liquids like methanol, acetone, carbon tetrachloride and n-propyl amine etc. A method has been standardised for the analysis of trace amounts of water in these liquids. Using quartz cells of 1 mm path length and the fundamental O-H absorption frequency at 3450 cm^{-1}, a detection limit of 100 ppm has been reached in the case of n-propyl amine. The major problem in achieving lower detection limits in this case arises from the possibility of ease of contamination at such low concentrations. Special precautions have to be taken to reduce contamination and further work is in progress in extending this method to the other liquids as well as to reduce the detection limit.

2. Infrared Non-dispersive Isotopic Analyser

(V.B. Kartha, N.D. Patel and P.K.S. Prakasa Rao)

Though the use of non-dispersive infrared analysis for process control, pollution detection, gas analysis etc. is well-known, it has never been recognised that the technique could be very advantageously used for isotopic analysis by infrared methods. We have recently designed a

system for the analyses of isotopic molecules by this method. The technique depends on the use of pneumatic detectors filled with the gas under investigation, these detectors responding to a chopped source of radiation. Depending upon the absorption of the gas in the detector, the detector can be made sensitive to any required isotopic component. So far the design of such pneumatic detectors have been empirical and involved a lot of trial and error methods. We have written a detailed computer programme to optimise the design of such detectors for any analytical requirement. The program computes the various parameters of the detector which will give a maximum response. One such calculation is illustrated in Fig.3, where the response is plotted as a function of pressure of the gas in the detector.

A suitable instrument has been designed and is being fabricated for analysis of ^{10}B - ^{11}B mixtures.

3. Boron Isotopic Analysis in Boric Acid

(V.A. Job, V.B. Kartha and S.B. Kartha)

An infrared method is being developed for the analysis of boron isotopes in boric acid. Conventional infrared spectra of the solid is not very helpful in this case because in the boric acid solid the isotopic bands overlap due to various broadening influences. Raman spectra technique also is not useful for isotopic analysis in this case, since the vibrational modes involving sufficient isotope shift do not appear or appear only weak, in the Raman spectrum. The broadening effects in the

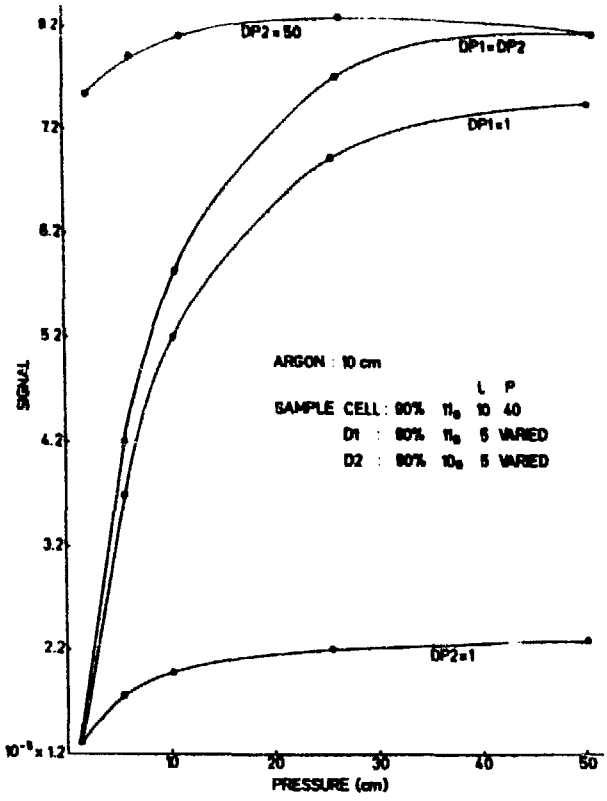

FIG. 3.

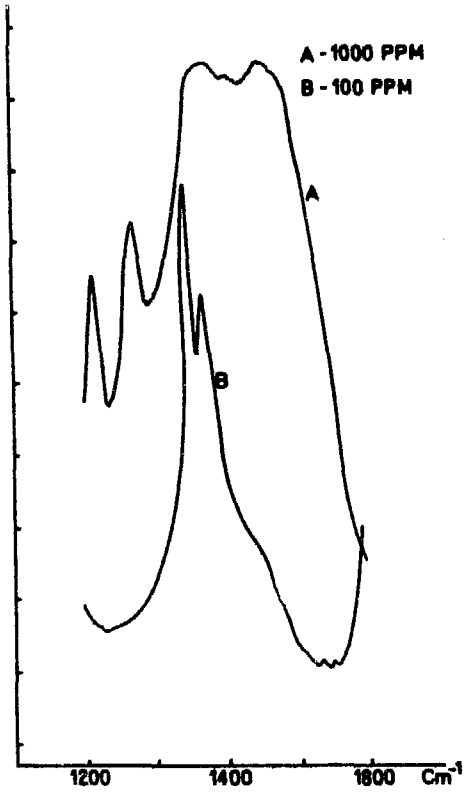

FIG. 4. H_3BO_3 IN KBr

solid could be reduced very much by incorporating the sample in a matrix, when at very low concentrations sharp absorption peaks are usually observed,[1] especially in alkali halide matrices involving the heavier ions. Spectra obtained with ppm quantities of boric acid in KI show isotope peaks which could be used for analysis. The effect of dilution on the 1500 cm^{-1} band is shown in Fig.4 from which it is obvious that at suitable dilutions the two peaks of ^{10}B and ^{11}B boric acid could be identified. The standardisation of a method for ^{10}B analysis based on these studies is under progress.

(1) V.B. Kartha, Proc.Nucl.Phys. & Solid State Phys.Symp. 14C, 375 (1972).

I(d) ANALYSIS OF GASES IN METALS

1. Determination of Oxygen and Nitrogen in Argon

(P.K. Wahi and S.S. Biswas)

Argon is widely used as an inert medium in industry for welding. The presence of trace amounts of oxygen in argon has deteriorating effects on the quality of the weld, particularly for aluminium and its alloys. In laboratory an inert medium may be needed for carrying out certain experiments. Argon is the only inert gas being produced in bulk indigenously. The gas has to be analysed for its oxygen and nitrogen contents, which are the most likely impurities.

The development of a sensitive β-ray ionisation detector of basic Sahin and Lipsky design (Fig.5) by us has prompted us to take up this development work. A 3 ft. long and $\frac{1}{4}$" O.D. copper tubing filled with 5A linde's molecular sieve and maintained at 60°C served as a column. About 3 ml of sample is fed into this column with the help of the sampling valve described below. At a flow rate of 60 cc/min. oxygen and nitrogen are eluted after 75 and 133 sec. respectively.

The gas chromatographic method developed is quick, simple and sensitive. The standard curves obtained are shown in Fig.6 and were drawn for the present assuming air to be consisting of only O_2 and N_2 in the sample ratio of 1:4. Microlitres of air were injected into the vacuum chamber filled with argon at NTP. The internal volume of the vacuum

chamber is 5:0 ml. The day-to-day variation in the sensitivity is negli-gible. However, curves drawn using different carrier gas cylinders (only of high purity Indian Oxygen make) show a change in sensitivity towards oxygen of about 10%, whereas the change in the nitrogen sensitivity is somewhat large. This is attributed to the change in the nitrogen content of different cylinders. The detection limits are 5 and 10 ppm for oxygen and nitrogen respectively.

Gas sampling valve: A six point piston-type gas sampling valve (Fig.7) was designed, fabricated and incorporated into the gas analyser. The valve is working satisfactorily. The neoprene 'O'-rings used are to be replaced periodically owing to the wear and tear.

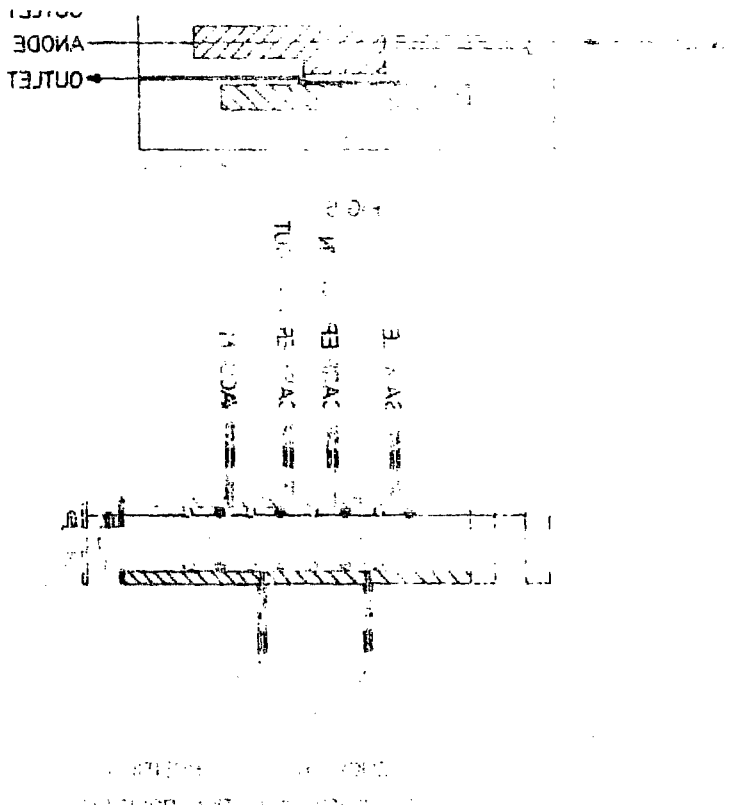

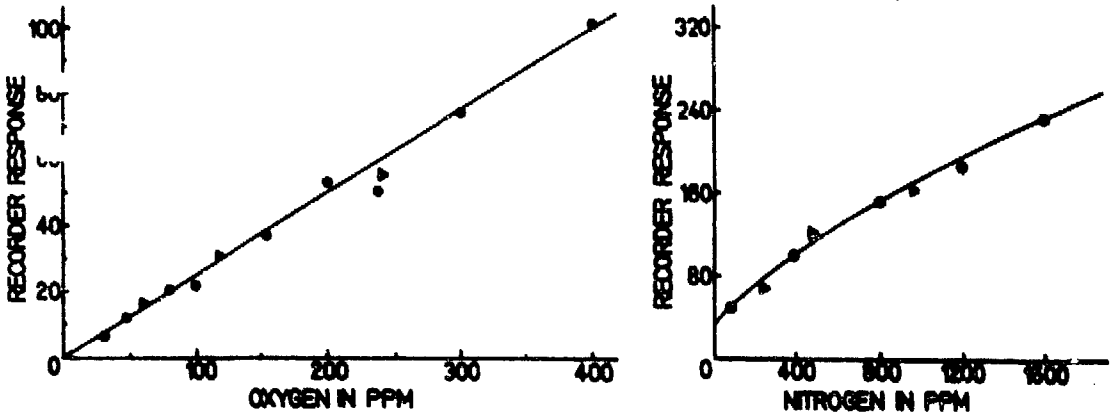

FIG.6.

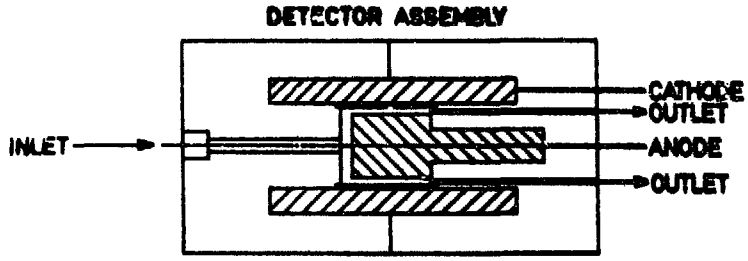

FIG.5

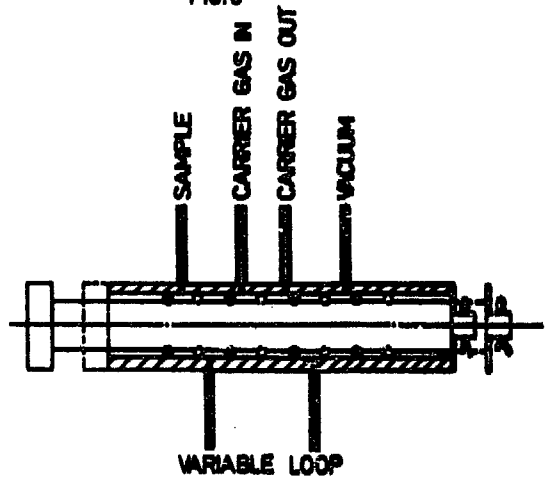

FIG.7.

N.B.

SOLID LINES SHOW BY-PASS POSITION

DOTTED LINES SHOW INJECTION POSITION

II. ATOMIC, MOLECULAR AND SOLID STATE SPECTROSCOPY

II(a) HYPERFINE STRUCTURE AND ISOTOPE SHIFT STUDIES IN ATOMIC SPECTRA

.. Isotope Shift Studies in Neodymium Spectra

(S.A. Ahmad and G.D. Saksena)

Isotope shift measurements in spectra of Nd with a view to obtain informations about the configurations involved in the particular transition was initiated by Rao et al[1] where $\Delta\nu$ (142-144) was investigated in 51 lines between the region 5200 - 5900 Å and almost all of them belonging to Nd I spectra. Ahmad and Saksena[2] studied isotope shifts $\Delta\nu$(142-144) in 306 lines of Nd I and Nd II which resulted in assignment of the isotope shift to various energy levels of Nd I and Nd II, and also configurations were suggested for various energy levels.

The present study is the continuation of the earlier work mentioned above. The isotope shifts have been recorded in 296 lines of Nd I and Nd II between 4710 - 5200 Å. Isotope shift data on earlier measurements are available only for 27 lines.

The above investigation was carried out on the Recording Fabry-Perot Spectrometer (REFPOS) described elsewhere[3]. The source was a liquid-air-cooled hollow cathode employing current between 16 mA and 32 mA, the carrier gas being He at 2.5 mm of Hg. The grating employed is a 15,000 lpi one, ruled over 10" x 4" area and blazed for 1.6 u. The Fabry-Perot plates were $\lambda/100$ and coated for maximum reflectivity at 5000 Å. Spacers of 10 mm ($\Delta\sigma$ = 501.48 mk) and 12 mm ($\Delta\sigma$ = 415.73 mk)

were used. All the lines were recorded with entrance and exit slits of 100 u width for monochromator recording and the same slit widths were us for recording the structure through Fabry-Perot interferometer.

The isotopic structures in the lines were recorded first with natural samples of Nd which consists of seven stable isotopes, A = 142, 143, 144, 145, 146, 148 and 150. All the lines were investigated with a single isotope Nd (A = 144) with 94.4% purity. This was done in order to establish whether the lines in question were single lines or more than one line. This helped in great way for analysis of the structure recorded with natural samples. Lines showing small isotope shifts were recorded with 28 mm spacer and enriched isotopes, ^{142}Nd (96.2%) and ^{144}Nd (94.4%).

The information deduced from the present study are briefly reported below. Throughout the discussion isotope shift stands for $\Delta\nu$ (142-144).

1. Although an extensive classification of Nd lines have been carried out by Wyart[4] there are still a good number of unclassified lines and only the wavelengths have been studied. The present study provides isotope shift $\Delta\nu$ (142-144) in 43 such unclassified lines. A good number of them may be due to transition $f^3d^2p - f^3ds^2$ as they show large values of isotope shifts. A few of them could be classified taking the energy levels of Blaise et al[5] and supplemented by our measurement of isotope shifts.

2. Isotope shifts have been measured in 109 classified lines of Nd I. The classification is due to Wyart[4]. The magnitude of isotope

shift varies between +40 to -110 mk. Most of the lines show large value of isotope shift showing that in this region most of the transitions are either of the $f^4dp - f^4s^2$ or $f^3d^2p - f^3ds^2$ type.

An interesting result has been obtained from the measurement of isotope shifts in the transition $f^4sp - f^4s^2$ in Nd I. As could be seen in Table I the ^5K (J = 5, 6, 7, 8, 9) terms of f^4sp show an isotope shift of -25 mk with respect to the f^4s^2 configuration whereas ^5I terms of f^4sp configuration show isotope shift of $\sim$ -10 mk with respect to the f^4s^2 configuration.

Table 1

ISOTOPE SHIFT FOR $f^4sp - f^4s^2$ TRANSITION INVOLVING ^5K_J AND ^5I_J TERMS

Energy levels in cm^{-1}			Wavelength	(142-144) 10^{-3} cm^{-1}	
				Present work	Earlier work (Ref.5)
$^5K_5^\circ$	20300.8	$^5I_4$ 0.0	4924.5152	- 31.6	- 31.7
$^5K_6^\circ$	21543.3	$-^5I_5$ 1128.1	4896.9201	- 21.2	- 22.4
$^5K_7^\circ$	22761.4	$-^5I_6$ 2366.6	4901.8385	- 29.8	
$^5K_8^\circ$	24212.4	$-^5I_7$ 3681.7	4891.0536	- 21.5	
$^5K_9^\circ$	25518.7	$-^5I_8$ 5048.6	4883.8098	- 35.5	- 38.8
$^5I_4^\circ$	20360.6	$-^5I_4$ 0.0	4910.0576	- 10	
	"	$-^5I_5$ 1128.1	5198.0537	- 10.2	
$^5I_5^\circ$	21005.4	$-^5I_4$ 0.0	4759.3412	0	
	"	$-^5I_5$ 1128.1	5029.4394	0	

3. There are only 24 lines which have been classified as Nd II and for which the isotope shift have been measured in the present study. The isotope shift $\Delta\nu$(142-144) in 5165.1261 Å is + 73.5 mk which is the highest positive shift reported for any of the Nd II lines. This shows that the level 24842.9 cm^{-1} is a f^3ds level. This being $f^3ds - f^4d$ transition gives the isotope shift of the level f^3ds 24842.9 as + 73.5 mk.

4. There are 33 new transitions which are not reported anywhere and have been found for the first time. They appear along with other 33 lines which are reported earlier and the wavelength separation with ^{144}Nd for most of the transitions are of the order of 0.028 Å which could be resolved in this case because of use of single isotope, photoelectric recording of signals and use of liquid-air-cooled hollow cathodes. The isotope shift in these lines have been measured using the "source exchange technique" with ^{142}Nd (96%) and ^{144}Nd (96%) in separate hollow cathodes. An example of this technique is given in Fig.8. The isotope shift values of these transitions will be helpful in their classifications.

5. The present study has provided isotope shifts for 109 energy levels of Nd I and also electronic configuration assignment has been made for many of these levels. Similarly isotope shift values for 19 energy levels of Nd II has been deduced and the configuration assignments made.

References

1. Rao, P.R., and Gluck, G., Proc. Roy. Soc. A 277 (1964), 540

2. Ahmad, S.A., and Saksena, G.D., (Under publication; also Annual Progress Report, Spectroscopy Division, 1972-73, p.57).

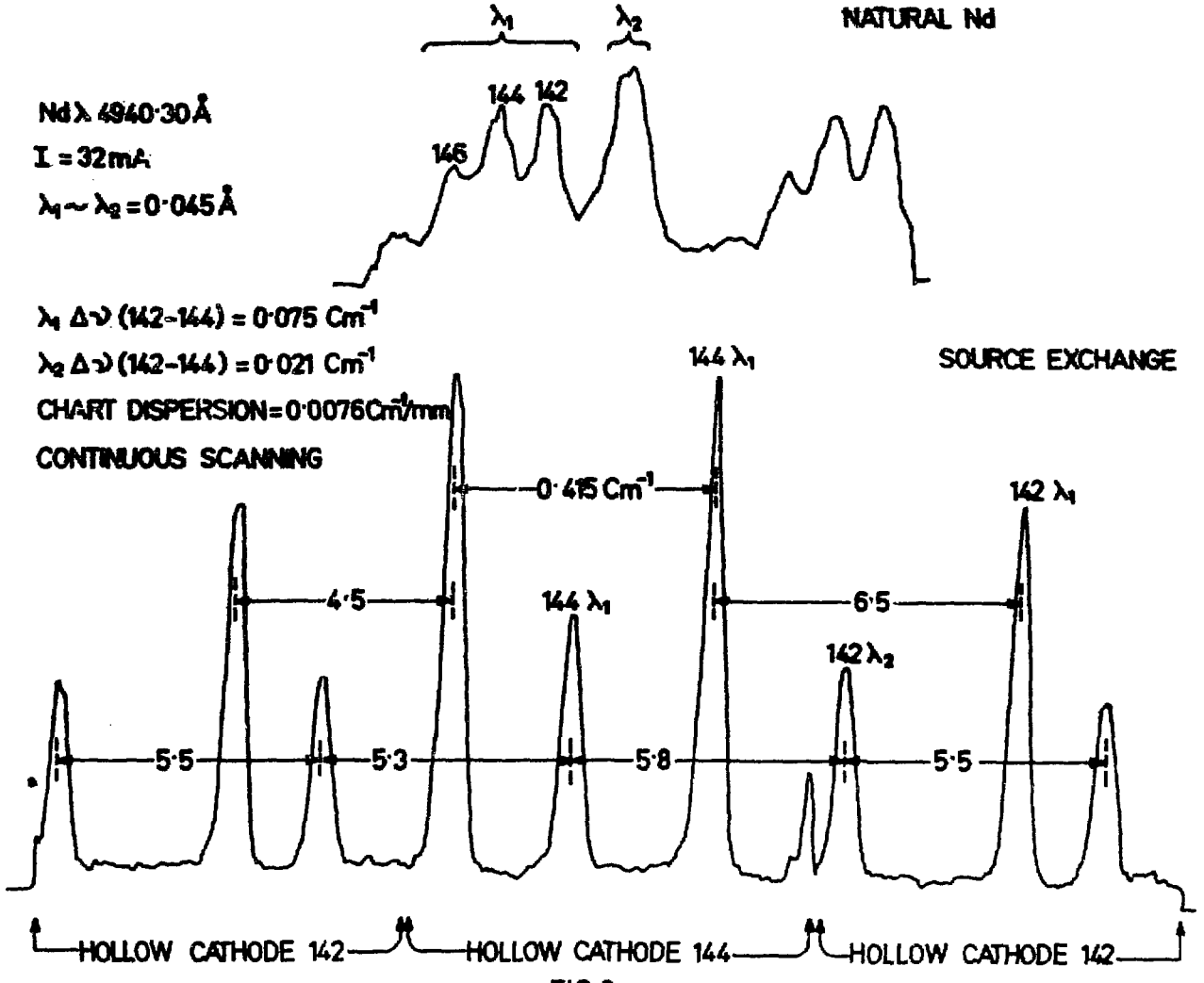
NATURAL Nd
λ1
λ2
Nd λ 4940·30 Å
I = 32 mA
λ1 ~ λ2 = 0·045 Å
144 142
146
λ1 Δν (142-144) = 0·075 Cm-1
λ2 Δν (142-144) = 0·021 Cm-1
CHART DISPERSION = 0·0076 Cm-1/mm
CONTINUOUS SCANNING
SOURCE EXCHANGE
144 λ1
142 λ1
0·415 Cm-1
4·5
144 λ1
6·5
142 λ2
5·5
5·3
5·8
5·5
HOLLOW CATHODE 142
HOLLOW CATHODE 144
HOLLOW CATHODE 142

FIG.8.

3. Saksena, G.D., and Ahmad, S.A., BARC-290 (1967).

4. Wyart, J.F., Thesis, University of Paris (1968).

5. Blaise, J., Cherillard, J., Verges, J., and Wyart, J.F., Spectrochemica Acta, 25B (1970), 333-381.

2. Isotope Shift Studies in Gadolinium Spectra

(S.A. Ahmad, A. Vemugopalan and G.D. Saksena)

Isotope shift in four lines in Gd I spectrum were reported by Klinkenberg[1]. Brix et al[2,3] studied isotope shifts in large number of lines of Gd I and Gd II spectra and evaluated the shifts in some electronic configurations of Gd. Kopfermann et al[4] investigated the isotope shifts in nine lines of Gd I between 5015 - 5617 Å and ten lines between 4092 - 4401 Å using samples enriched in all the even isotopes of Gd.

The present work was undertaken to make a more detailed study of isotope shifts involving ^{156}Gd and ^{160}Gd. The isotope shift (IS) $\Delta\nu$ (160 - 156) measurements have been carried out in 130 lines in Gd I and Gd II spectra between 3930 - 4140 Å. Isotope shift data on earlier measurements are available only for nine lines in this region. Many of them have been classified by Russel[5] and by Van Kleef et al[6]. However, with the help of energy levels listing of Blaise et al[7] and the present isotope shift measurements, it was possible to classify a number of additional lines in the spectra of Gd I and Gd II.

The above investigations were carried out on the Recording Fabry-Perot Spectrometer described elsewhere[8]. The experimental details are the same as given there except that the Fabry-Perot plates were coated for maximum reflectivity at 4300 Å. A 10:7 mixture of ^{160}Gd (95.5%) and ^{156}Gd (93.6%) with a 12 mm ($\Delta\sigma$ = 415.73 mK) spacer was used for recording IS in all the lines. Whenever more than two components (one each due to 160 and 156 isotopes) appeared in the structure of the line (see Fig.9) it was recorded with a single isotope ^{160}Gd (95.5%) and with 10 mm ($\Delta\sigma$ = 501.48 mK) and 12 mm spacers. Lines showing small IS were investigated with 28 mm spacer.

From the present study, it has been possible to deduce the following informations.

1. It has been suggested that the variation in isotope shift (IS) (160-156) values in different terms of f^7d^2p configuration, i.e., ^{11}G(J = 1, 2, 3, 4, 5, 6, 7) terms are due to configuration mixing with the ^{9}D(J = 2, 3, 4, 5, 6) terms of f^7dsp configuration, as there are variations in IS values of ^{9}D(J = 2, 3, 4, 5) terms also. They both combine with the common f^7ds^2 configuration.

2. f^8ds configuration has only been recently reported by Blaise et al[7] and no earlier IS data is available for this configuration. Our data on IS for $f^8ds - f^7ds^2$ transition shows that there is a large screening factor involved for the eighth f-electron, and it has been deduced that $\frac{\zeta(4f^7 5d6s)}{\zeta(4f^8 6s)} = 1.8$, which is closer to the value of 1.9 suggested by Blaise and Steudel[9] for $\frac{\zeta(4f^6 5d6s)}{\zeta(4f^7 6s)}$ for Eu II.

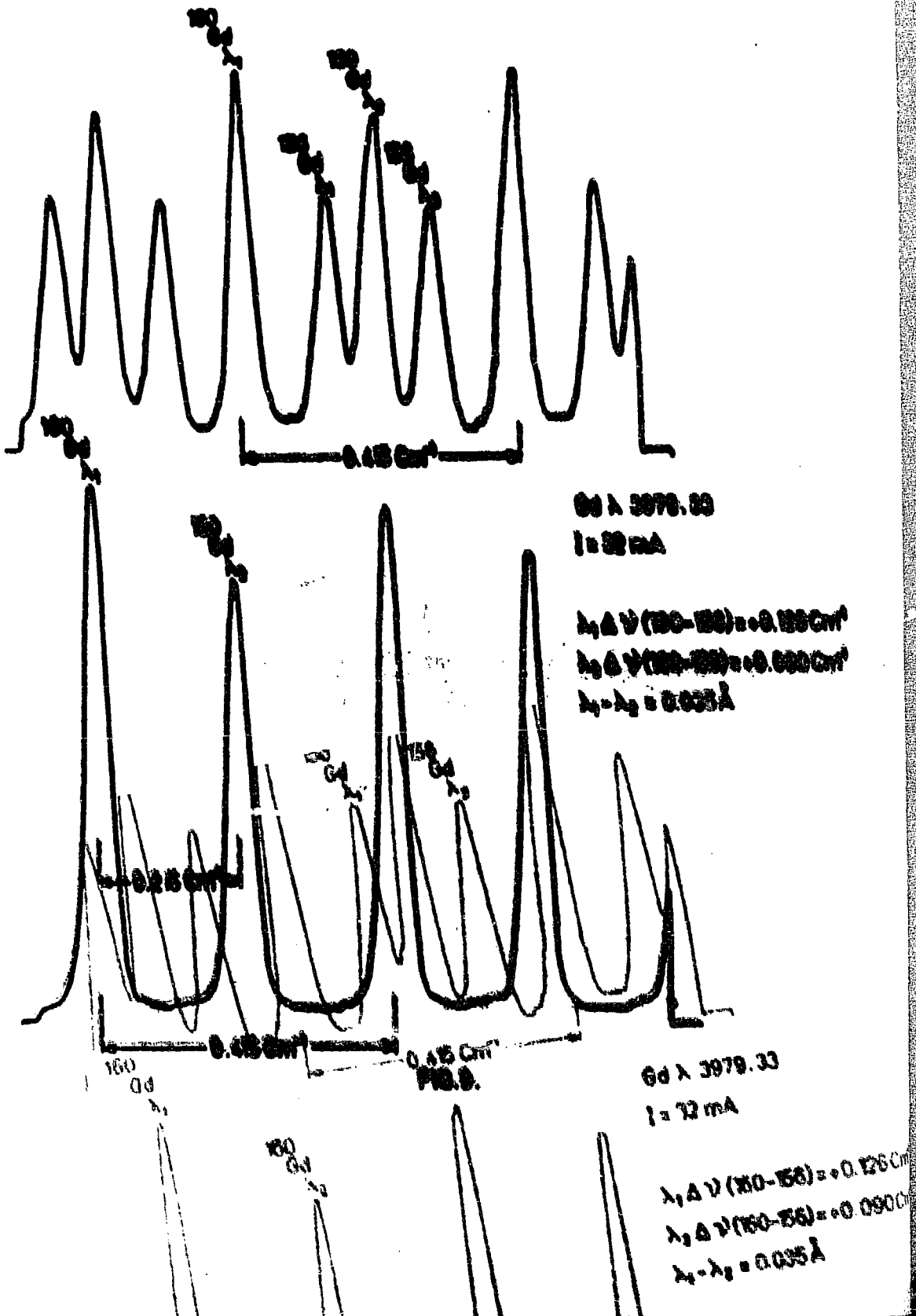

FIG. 8.

3. This is the first study which reports negative IS values in case of Gd. The negative shifts are expected only in case of Gd II lines and usually they are very weak in intensity in hollow cathode spectra. [illegible] with REFPOS it was possible to record IS in these weak lines. The highest negative shift is of the order of -70 mK for ^{160}Gd and ^{156}Gd for $f^8p - f^8s$ transition.

4. The usefulness of IS in deciding about the configuration is evident from the data in Table I, which gives the isotope shifts in the energy levels which all combine with f^7ds^2 configuration. As can be seen, the suggestion of Russel[5] that these energy levels form a multiplet originating from f^7dsp configuration is erroneous as only two energy levels 32020.38 cm^{-1} and 31847.51 cm^{-1} show large enough isotope shift to be f^7dsp. The energy levels 31999.82 cm^{-1}, 32149.55 cm^{-1} and 32251.80 cm^{-1} show similar isotope shift and the g-values as reported by Blaise et al[7] has made us to suggest that they are $^5P_3$, $^5P_2$ and $^5P_1$ terms respectively and they originate from f^7dsp configuration.

References

1. Klinkenberg, P.F.A., Physica 12, (1946), 33.
2. a) Brix, P., Z. Physik 132, (1952), 579.
   b) Brix, P., and Bugler, H.D., Z. Physik 133, (1952), 362.
3. Brix. P., and Lindenberger, K., Z. Physik 141, (1955).
4. Kopfermann, H., Kruger, L., and Steudel, A., Ann.Physik 20, (1957), 258.
5. Russel, H.E., JOSA 40, (1950), 550.
6. Van Kleef, Th. A.M., Blaise, J., and Wyart, J.F., J. de Phys. 32 (1971),609
7. Blaise, J., Chevillard, J., Verges, J., and Wyart, J.F., Spectrochim. Acta 26B, (1971), 1.
8. Saksena, G.D., and Ahmad, S.A., BARC-209 (1967).
9. Blaise, J., and Steudel, A., Z. Physik 209, (1968), 311.

Table 1

Energy levels (cm^{-1})	Russel[5] Term and configuration.		Blaise et al[7] Term and configuration.		$g_{obs.}$	Present studies I.S. (160-156) (for transitions to f^7ds^2).	Suggested term and configuration	
31794.80	f^7dsp	$^7F_6$	-	J = 6	1.485	+ 106.9 mK	f^7dsp confirmed	
32020.38	"	$^7F_5$	f^8ds	$^7F_5$	1.540	+ 123.3	f^8ds "	
31847.51	"	$^7F_4$	f^8ds	$^7F_4$	1.500	+ 128.7	" "	
31999.32	"	$^7F_3$	-	J = 3	1.575	+ 109.7	f^7dsp $^5P_3(g_{th.}$ 1.666)	149.794 cm^{-1}
32149.55	"	$^7F_2$	-	J = 2	1.700	+ 108.6	" $^5P_2(g_{th.}$ 1.833)	102.185 cm^{-1}
32251.80	"	$^7F_1$	-	J = 1	2.230	+ 102.3	" $^5P_1(g_{th.}$ 2.500)	
32341.16	"	$^7F_0$	-	J = 0	-	+ 99	" -	

II(b) SPECTRA OF RARE EARTH IONS IN CRYSTALS

1. Spectroscopic Studies on Trihydrated Neodymium Trichloroacetate

(R.C. Naik and K.H. Ayyar)

Previous spectroscopic studies[1] carried out in our laboratory on the rare earth trichloroacetates of Eu, Tb, Pr and Nd have shown that there exists a new phase for these complexes with two molecules of water of hydration, which was not known previously. For identifying the different states of hydration, selected groups of absorption and fluorescence spectra of the particular complex were used. In case of Eu-trichloroacetate, however, a detailed study of the absorption and fluorescence spectra were made which showed that the site symmetry around the rare earth ion in Eu-trichloroacetate is very low and is likely to be C_2 or C_s.

As an extension of these studies, a detailed investigation of the trihydrated phase of the Nd-trichloroacetate was undertaken. The absorption spectrum of this complex consists of groups of sharp lines extending from near infrared to ultraviolet region till ligand absorption sets in below 2800 Å. The groups of sharp line spectra, as is well-known, arise due to forbidden transitions between the energy levels of the $4f^3$ configuration of Nd^{3+} ion. A detailed study of the absorption spectra of Nd^{3+} in Nd-trichloroacetate can not only tell about the symmetry and strength of the crystal field about the rare earth ion but can also give information regarding the spin-orbit coupling, degree of co-valency,

nephelauxetic effect etc. in the complex under study. Establishing the energy levels of the rare earth ion viz, Nd^{3+}, from the absorption spectra is the first step in such studies.

Absorption spectra were recorded at 77°K between 4000 - 9000 Å using a Steinheil spectrograph with medium optics and also a Jarrel Ash grating spectrograph with a 15,000 lines/inch grating blazed at 4000 Å. Single crystals grown from an aqueous solution of Nd-trichloroacetates, and sealed in a vycor tubing with a few cm of helium were used for all absorption studies. The various absorption groups observed between 4000 - 9000 Å have been assigned to different electronic transitions of the Nd^{3+} ion. In order to locate the higher Stark levels of the ground state, a knowledge of which is quite essential for locating the Stark levels of the excited states from the absorption spectral studies, spectra were recorded by varying the temperature of the sample between liquid nitrogen and room temperature. The most unambiguous information regarding the ground state splitting came from the transition $^2P_{\frac{1}{2}} \rightarrow {}^4I_{9/2}$. In this case, the excited $^2P_{\frac{1}{2}}$ state with $J = \pm \frac{1}{2}$ does not split under a crystal field and therefore consists of a single level. Hence the additional lines which appeared at higher temperature could be assigned to higher Stark levels of the ground state, viz, $^4I_{9/2}$. Analysis of the full absorption spectrum to establish the Stark fine structure of individual J levels of Nd^{3+} in $Nd(CCl_3COO)_3.3H_2O$ and the calculation of the Slater parameters, F_2, F_4, F_6 and the spin-orbit coupling constant is in progress.

---

1. R.C. Naik and K.H. Ayyar, Annual Progress Report 1972-73 (BARC-684), Spectroscopy Division, p.62-65.

II(c) SOLID STATE SPECTRA - LUMINESCENCE

1. The Design of a Vacuum Ultraviolet Monochromator

(J. Ramamurty)

For the study of optical properties of solids below 1850 Å, one needs a vacuum ultraviolet monochromator. We have designed an instrument with low dispersion which can be used for low resolution studies. The details of this instrument and considerations on which mechanical parts are laid out are given below.

The mounting chosen is Richardson Tousey type. In this the entrance and exist slits are fixed on the Rowland circle and the grating moves on the Rowland circle. The angle of emergence of the diffracted beam at the exit slit therefore changes with wavelength.

Fig.10 shows the optical layout of the instrument. The outline of various mechanical parts are also shown in the figure. The grating is fixed at the end of an arm with provision for adjustments of the plane of the grating. The arm is fixed on the main flange and provided with bearings. Scanning is done by rotating the arm about the centre of the Rowland circle by pushing it by a wedge. The wedge rides on a screw rotated by a motor from outside the vacuum chamber. The vacuum in the chamber during scanning is maintained by O-ring seals. The instrument is focussed when entrance and exit slits and the centre of the grating all lie on the Rowland circle. To achieve this, provision is made for moving the entrance and exit slits along the central optical line (as defined below) without disturbing the vacuum by mounting the slits on telescopic tubing with

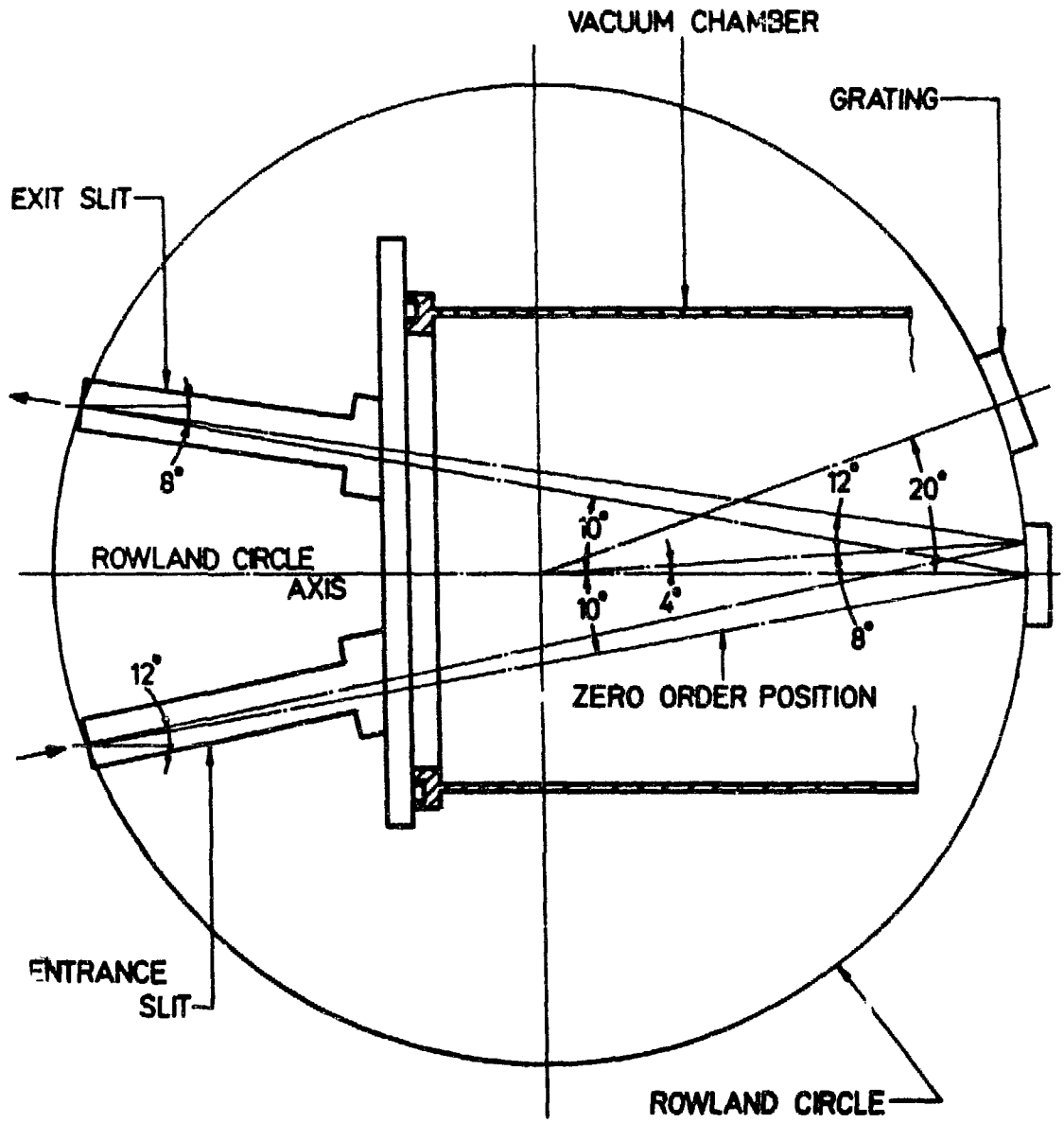
VACUUM CHAMBER
GRATING
EXIT SLIT
8°
ROWLAND CIRCLE
AXIS
10°
10°
4°
12°
20°
8°
12°
ZERO ORDER POSITION
ENTRANCE
SLIT
ROWLAND CIRCLE

FIG.10.

O-ring seals.

Since the grating moves along the Rowland circle, the intensity of radiation falling on the grating changes with wavelength. The range for which the instrument is normally used is 500 to 2300 Å. The intensity of illumination is maximised in the present case for an intermediate wavelength of 1145 Å. The intensity of radiation emerging from the discharge tube will be maximum along the axis of the discharge tube. When the grating is set for 1145 Å, the central incident ray and the axis of the discharge tube (and hence the axes of the telescopic slit holders) are coincident. The principal ray in this position of the grating defines the central optical line mentioned above. The telescopic slit holders are therefore not placed symmetrically with respect to the main flange.

Let be the angle of rotation of the grating arm as shown in the figure. The angle of incidence (i) and diffraction (φ) in the zero order are 10°.

$$\therefore \quad i + \varphi = 20^\circ , \qquad i = 10 - \frac{\theta}{2} , \qquad \varphi = 10 + \frac{\theta}{2}$$

The grating equation in first order is:

$$\begin{aligned} \lambda &= d\,(\sin i + \sin \varphi) \\ &= 2d \sin \frac{i - \varphi}{2} \operatorname{Cos} \frac{i + \varphi}{2} \\ &= 2d \sin \frac{\theta}{2} \operatorname{Cos} 10 \\ &= 2\,(.98481)\,\frac{1}{600} \operatorname{Sin} \frac{\theta}{2} \text{ m for a grating with 600 l/mm} \\ &= 32827 \sin \frac{\theta}{2} \text{ A units} \end{aligned}$$

A[illegible]s expression gives the output wavelength as a function of rotation o[illegible]ngle of grating on the Rowland circle. The values of the output wavelength for 4° and 8° rotation of the grating are 1145 Å and 2290 Å respectively.

The central optical line, therefore, corresponds to a rotatio of the grating by four degrees from the zero order. In this position the inclination of the axes of the telescopic tubings carrying the entrance and exit slits are 12° and 8° respectively to the tube axis (axis perpendicular to the main flange). The radius of the Rowland circle is 20.03 cm. and the reciprocal linear dispersion at the exit slit is 41 Å/mm.

The system is designed for use with a windowless discharge tube. The liquid nitrogen trap diffusion pump, valve, etc. are mounted on the main chamber. All these can be pushed on rails to have access to the grating mount, arm, drive, carriage for cleaning, alignment, etc.

II(d). ELECTRONIC SPECTRA AND STRUCTURE OF FREE RADICALS AND SIMPLE MOLECULES

1. Reinvestigation of the Band Systems of NS

(T.K. Balasubramanian and N.A. Narasimham)

In continuation of the reinvestigation of the γ and the β-systems of the NS[1] (which was taken up in order to resolve the discrepancy between microwave and optical spectroscopic data) and analysis of the 0-1 band of the γ-system has been completed. A close examination of the 0-0 band revealed a breaking off of the Q_{11} and P_{22} branches suggesting that rotational levels with F_2 ($N \gtrsim 58$) and F_1 ($N \gtrsim 67$) belonging to the $v = 0$ level of the initial ^{2} state are predissociated. Although the 0-1 band is much stronger than the 0-0, its analysis could not provide any confirmatory evidence on the predissociation, as the "last lines", crucial for the confirmation, were badly overlapped. It is proposed to take up the analysis of the much weaker 0-2 band. The predissociation provides a useful upper limit of $De \lesssim 46204$ cm^{-1} for the dissociation energy of NS.

The analysis of the 0-0 band of the β-system has now been completed and revised rotational constants for the initial $^2\Delta$ state have been derived. Both F_1 and F_2 rotational terms of the $v = 0$ level of the $^2\Delta$ state seem to be perturbed, the F_2 terms rather severely, for J values below 33.5 and hence could not be described by the usual $^2\Delta$ formulae. For $J \gtrsim 33.5$, however, the perturbation apparently ceases and both F_1 and F_2 could be fitted to the appropriate formulae. The value of $B_0 = 0.6964_2$ cm^{-1} thus derived differs significantly from the value 0.6925 cm^{-1} reported by Barrow et al[2].

Also, the present analysis has, for the first time, enabled a quantitative evaluation of the coupling constant A_0 of the $^2\Delta$ state. It is proposed to study the other bands of the system which might provide further clues in the analysis of the perturbation.

(1) T.K. Balasubramanian and N.A. Narasimham, J.Mol.Spectroscopy (Accepted for publication).

(2) R.F. Barrow, G. Drummond and P.B. Zeeman, Proc.Phys.Soc.London 67A, 365 (1954).

2. Absorption Spectrum of CS_2

(C.G. Mahajan* and G. Lakshminarayana)

In the vacuum ultraviolet carbon disulphide has a very strong absorption band system in the 2200-1800 Å region followed by a progression of diffuse bands extending from 1750-1650 Å. Another strong absorption system lies in the 1625-1500 Å region. Detailed vibrational analysis of the last system has not been done so far. With the view to investigate this system (almost along the lines Kleeman did on CS_2) we undertook to scan the CS_2 absorption in the vacuum ultraviolet region (2200-1500 Å).

(A) 2200-1800 Å System

This strong system, firstly photographed by Price and Simpson(1) was shown to consist of a single progression with a frequency difference of 410 cm^{-1} (varies between 390 and 430 cm^{-1}) corresponding to the excitation of the totally symmetric stretching mode, ν_1 which has a value of 658 cm^{-1} in the ground state, $^1\Sigma_g^+$. Ramasastry and Rao(2), besides the strong progression, observed some weak bands and assigned these bands to a progression

* DAE Junior Research Fellow

involving the transition $(v,2,0)' \quad (0,0,0)''$. Douglas and Zanon[3] photographed a part of this system (above 2100 Å) on a high dispersion spectrograph (plate factor varied between 0.35 and 0.23 Å/mm). They analysed the bands partially, and found that most of the bands above 2100 Å were hot bands corresponding to the excitation of antisymmetric bending mode, ν_2. From isotopic studies they established that the molecule is strongly bent in the excited state and designated it to be a $^1B_2$ state.

We observed these bands while scanning the S_2 absorption spectra (for experimental details, please refer "Rydberg Transitions of S_2" given elsewhere in the Report).

We photographed this system at various pressures and observed that each strong band of P and S (Price and Simpson) progression is always accompanied by about equally intense band lying on the longer wavelength side. In our plates bands are observed only upto 47982 cm^{-1}. Probably, the CS_2 molecules in the absorption cell were too small to photograph the very weak bands lying in the region 45950 to 4761 cm^{-1}. On arranging the new bands we get a progression of frequency 392 cm^{-1} (varying between 379 and 410 cm^{-1}). Band head data of all the bands observed in the present work together with those of P and S, Ramasastry and Rao, and Douglas and Zanon together with their assignments are given in Table I. New bands arranged in a progression are given in Table II.

The new bands could not be observed without the appearance of the P and S progression and vice-versa. That is both the progressions appear, without fail, simultaneously. In addition, their intensities are more or

less equal and the new bands are lying on the longer wavelength side of the red degraded bands reported by P and S, these new bands, very probably are the sub-band heads forming a part of the rotational structure of the main progression corresponding to the excitation of totally symmetric stretching mode ν_1.

TABLE I

Present work	Price & Simpson		Ramasastry & Rao	Douglas & Jones[a]		
ν (cm^{-1})	ν (cm^{-1})	I	ν (cm^{-1})	ν (cm^{-1})	I	Assignment
-	45950	00	45952	45943.0	S	Σ_4^1
				45958.6	S	π_3^1
-	46370	0	46368	46371.4	S	π_2^1
-	46790	0	46762	46761.5	S	Σ_2^1
				46767.9	S	π_1^1
				46788.0	M	π_3^h
-	47200	1	47170	47150.0	S	Σ_0^f
				47182.7	S	π_1^1, Σ_2^h
				47207.4	M	—
-	47610	1	47599	47600.2	M	π_1^h
47982	48020	2	47981	47982.8	S	Σ_0^h
48067			-	48070.6	S	—
48445	48440	3	48460	48447.5	S	—
48477	-	-		-		
48875	48870	5	48862	-		
49279	49290	6	49274	-		
49674	-		49693	-		
49710	49710	7				
50062	-		50098	-		
50109	50110	7				

TABLE I(Contd.)

Present work	Price & Simpson		Ramasastry & Rao	Douglas & Zanon[a]		
$\nu(cm^{-1})$	$\nu(cm^{-1})$	I	$\nu(cm^{-1})$	$\nu(cm^{-1})$	I	Assignment
50441	-		-	-		
50478	50480	8	50477	-		
50794	q -		-	-		
50840	-		-	-		
50869	-		-	-		
50896	50900	9	50909	-		
51221	-		-	-		
51271	51280	10	51285	-		
51608	-		-	-		
51709	51720	8	51730	-		
51996	-		-	-		
52111	52140	7	-	-		
52431	-		-	-		
52785	-		-	-		

(a) The bands are designated as Σ, Π, Δ, according to value of $\lambda = k = 0, 1, 2, \ldots$. The superscripts a,b,c,... designated excited state and its subscripts 0,1,2, ... is the vibrational quantum number V_2 of the lower state.

S = Strong, M = Medium, W = Weak.

Refer to the intensity of a band compared with its close neighbours.

TABLE II

$\nu(cm^{-1})$	ΔG
48067	410
48477	398
48875	404
49279	395
49674	388
50062	379
50441	399
50840	381
51221	387
51608	382
51990	

(B) 1600 Å System

Another strong system, photographed by Price and Simpson[1] lies in the region 1625-1500 Å. This system consists of condensed groups of sharp bands and each group shows well resolved structure. The structure of each group was attributed to the rotational structure assuming that the molecule becomes slightly bent in the excited state.

We photographed these bands in the conventional way, that is, keeping an absorption cell ~ 30 cm long, 2.5 cm diameter pyrex tube between the continuum source and the spectrograph. CS_2 vapour enter into the absorption cell from its one end and are being continuously pumped out from the other end. We photographed these bands under different experimental conditions, using Xe continuum as the background, on a 3-meter normal incidence concave grating vacuum spectrograph. SWR plates were used.

In addition to the bands reported by Price and Simpson, we have observed many more bands. It was observed that with the increase of pressure, the group of bands at $\lambda \approx$ 1612 Å, 1595 Å look like patches and the number of bands in each group is increased. The gross structure of the system indicates that both the totally symmetric stretching mode, ν_1 and antisymmetric bending mode ν_2 are excited in adherence to the vibrational selection rules, viz,

$V = 0, \pm 1, \pm 2, \ldots$ ---------- for totally symmetric vibration.

$V = 0, \pm 1, \pm 2, \ldots$ ---------- for antisymmetric vibration.

A relatively week group of bands at 1577 Å having a separation of 1620 cm^{-1} from the main band at 1595 Å is assumed to be corresponding to the anti-symmetric stretching mode, ν_3 which has a value of 1532 cm^{-1} in the ground state. Truly speaking, this is a forbidden transition. This transition may be, as put forth by Price and Simpson, explained assuming that the dissymmetry is induced in the molecule by the excitation of SCS to SCS* in analogous to SCO. This makes the symmetries of both the stretching modes equivalent.

Assuming the molecule retains its linearity in the excited state and with the help of Kleman's[4] ground state data, we could partially analyse the bands into sequences $V = 0, \pm 2, \ldots\ldots\ldots$ corresponding to the excitation of bending mode, ν_2. Though Boltzmann factor prevents such sequences, the intensity variations with pressure supports our analysis. Only the main diagonal of Deslandres table (i.e. sequence $V_2 = 0$) could be fitted undoubtedly which is in agreement with the Franck-Condon principle[5], viz, $V = 0$ is the most intense sequence and the intensity decreases very rapidly with increase of V_K where V_K is the antisymmetric vibrational quantum number.

Band head data of all the bands and the tentative assignments of some of the bands together with Price and Simpson values are given in Table III.

TABLE III

Present work (cm^{-1})	Price and Simpson (cm^{-1})	Assignment
61734		
61860	61865	
61910	-	
61955	61960	
62012	62017	
62079	62080	
62342	-	
62385	-	000 - 010 Forbidden transition
62407	-	
42454	-	040-040
62540	62550	030-030
62620	62626	020-020
62700	62702	010-010
-	62754	
62774	62774	000-000
63110	-	140-040
63204	63204	130-030
63267 63312	63287	120-020
63360	63360	110-010
63430	63430	100-000
43450	63448	
63490	63512	
63535	63550	
64123	-	
64272	-	021-020
64283	-	
64324	64324	011-010
64398	64398	001-000
64421	64416	

TABLE III (Contd)

Present work (cm^{-1})	Price and Simpson (cm^{-1})	Assignment
64445	64452	
64757		
64827		
64885		
64955		
64979		111-010
65049		101-000
65120		
65132		
65202		
65261		
65427		
65486		

The excited state vibrational constants derived from our analysis, together with their corresponding values in the ground state are listed in Table IV.

TABLE IV

Excited state	Ground state
ν_1 = 656 cm^{-1}	657.98 cm^{-1}
ν_2 = 324 cm^{-1}	396.7 cm^{-1}
ν_3 = 1624 cm^{-1}	1532.5 cm^{-1}

References

1. W.C. Price and D.M. Simpson, Proc. Roy. Soc. London, 165A, 272 (1938)
2. C. Ramasastry and K.R. Rao, Ind. J. Phys., 21, 318 (1947).
3. A.E. Douglas and I. Zanon, Can. J. Phys. 42, 627 (1964).
4. B. Kleman, Can. J. Phys., 41, 2034 (1963).
5. G. Herzberg, Molecular Spectra and Molecular Structure, Vol.III, (D. Van Nostrand, 1966), pp.152.

---

3. Reinvestigation of Rotational Structure of O_2^+ Bands

(G.L. Bhale)

The 5-3, 6-3, 7-2 and 8-2 bands of the second negative ($A\,^2\pi_u - X\,^2\pi_g$) band system of O_2^+ were photographed under high resolution and dispersion on a 3.4 metre Ebert grating spectrograph. These were then analysed for their rotational structure. It was found that the spin-orbit coupling constant A of the upper state has negative sign for $v' < 5$. However, for $v' \geqslant 6$, A was seen to be positive.

In addition to this, the splittings of the Λ-doublets in the upper state $A\,^2\pi_u$ were carefully studied. Earlier workers did not carry out these investigations and hence the spin-splitting constant γ, which represents the magnetic interaction between Λ and S was not determined. Recently, Albritton et al (1973)[1] subjected the entire high resolution data of previous workers to a non-linear least-squares fit and obtained a complete set of molecular constants. But significantly, γ was omitted in their calculations too.

Present investigations indicate that the observed splittings of the R-doublets can be explained only if the constant γ is introduced. Value of this constant has been determined graphically for all the v' levels involved.

(1) D.L. Albritton et al, J.Mol.Spectrosc. 46, 89 (1973).

4. Rare Gas Continuum Sources

(G. Lakshminarayana and C.G. Mahajan*)

To study the absorption of atoms and molecules in the vacuum ultraviolet, hydrogen emission continuum (5000-1700 Å), Lyman continuum (7000-300 Å) and the Hopfield continuum (1100-600 Å) were being commonly used in the past as the background. As hydrogen continuum is limited to 1700 Å (below 1700 Å molecular hydrogen many line spectrum comes up), there was no continuum source known except the Lyman continuum of hydrogen in the region from 1700 Å to 1100 Å till mid-fifties. While Lyman continuum has the advantage that it may be used in any region right from 7000 Å down to 300 Å, its disadvantages, viz., difficulty to use in the higher orders, rapid wearing of capillary and hence its frequent replacement, many impurity emission lines and the irregular intensity distribution, the most serious disadvantage, limit its use as the background.

In order to have an easily excited and clean continuum, Tanaka and others[1,2] had photographed the rare gases continuum excited either by a microwave discharge or mildly condensed transformer discharge and are now being commonly employed for photographing the absorption spectra in the

* DAE Junior Research Fellow

vacuum ultraviolet region. The useful ranges of these continua are given in Table I.

TABLE I

Gas	Useful range (Å)	Pressure used (torr)
He	1100-600	40
Ar	1500-1100	180
Kr	1800-1250	180
Xe	2000-1500	180

We have made in our laboratory these rare gas continua sources and are being routinely used to investigate the absorption of various molecules.

(A) Argon, Krypton and Xenon Continua

As all these continua have a very close resemblance with respect to their appearance, except their ranges and method of excitation, a common type of discharge tube is used. The discharge tube, 18 cm long capillary having a bore of 2.5 mm provided with two aluminium electrodes, was well cleaned and baked thoroughly for six to seven hours. The discharge tube is filled with a spec-pure rare gas after passing through liquid nitrogen, allyl alcohol, and dry ice cooled trap for argon, krypton and xenon gas respectively, to a pressure of ~180 torr. A transformer 15 kV, 17 mA, together with a small condenser (0.005 μF) was used for the mildly condensed transformer discharge excitation of these continua. A 3-meter normal incidence concave grating vacuum spectrograph and Kodak SWR plates were used to

photograph the continua. Fig.11 shows a photometric trace of these continua.

As our aim was limited to produce the various continua for the molecular absorption studies we did not go in detail as to their appearance and variation of intensities with respect to pressure in the discharge tube.

Tanaka[2] has observed several emission and absorption bands coming up along with these continua. In the case of krypton, Tanaka[2] has reported five absorption bands at λ = 1247.6 Å, 1246.1 Å, 1244.8 Å, 1243.7 Å, 1242.5 Å and one emission band at 1327 Å. In our plates the absorption bands, probably because of high pressure we used, are so strong that they merge into one another to form a continuous absorption patch (1250 - 1225 Å). And besides the emission bands at λ = 1327 Å reported by Tanaka, we have observed six more diffuse emission bands lying on the shorter wavelength side of the krypton resonance line λ = 1236 Å. As these bands appear along with the krypton continuum only, the carrier of these bands is assumed tobe krypton molecule. Their band head data are given in Table II.

TABLE II

(Å)	(cm^{-1})
1223.51	81732
1219.03	82032
1207.83	82793
1193.27	83803
1192.16	83881
1172.19	85310
1158.27	86335

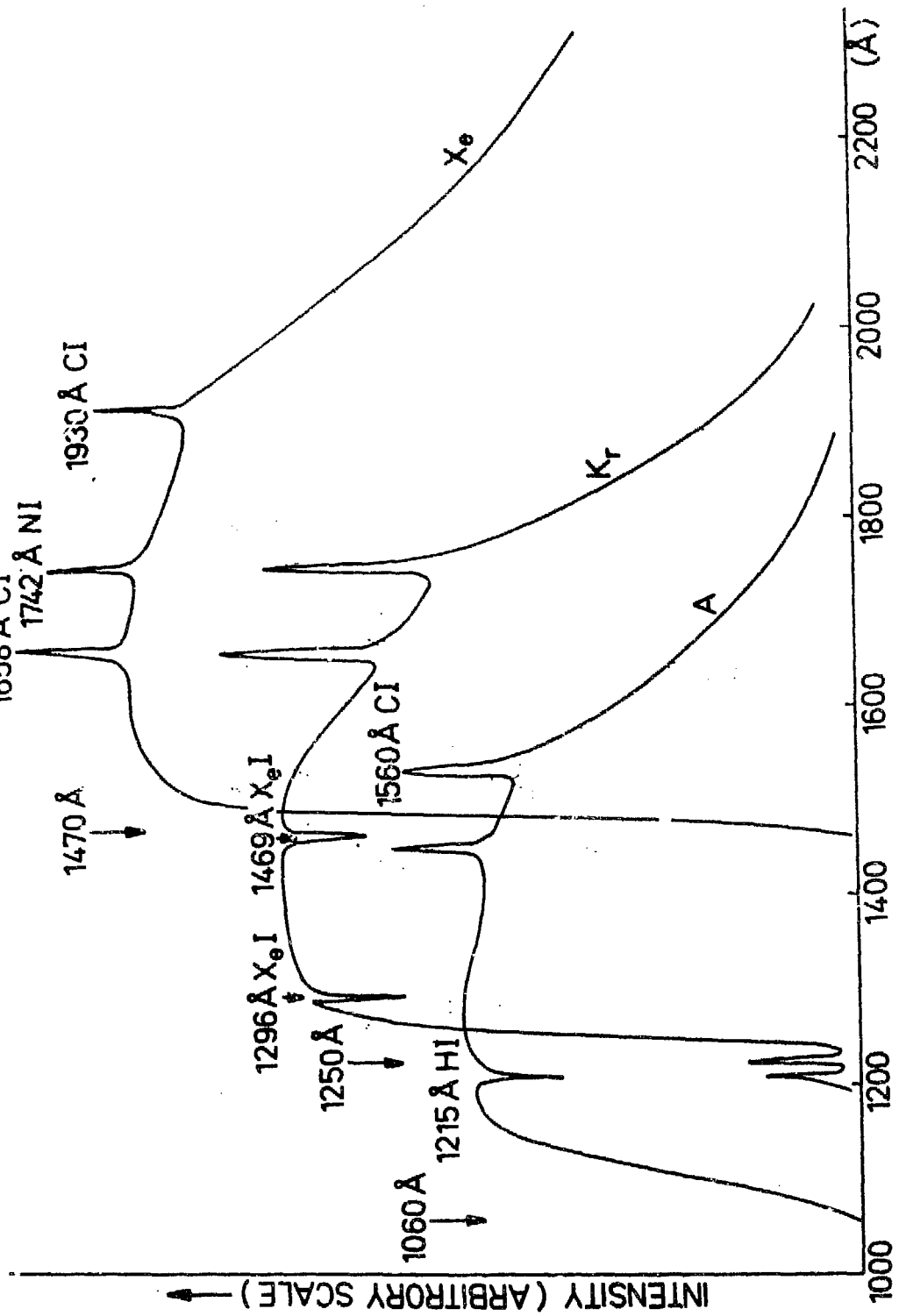

FIG.11. RARE GAS CONTINUA

(B) Hopfield Helium Continuum[3,4]

Since no known material transmits in the helium region (1100-600 Å) the light radiation should go directly on to the grating from the discharge tube. This continuum is most efficiently produced in a mildly condensed discharge through continuously flowing highly purified helium gas at a pressure of 40 torr. This requires the running of discharge in a tube that is separated from the spectrograph by a series of slits of varying widths. That is by setting up a differential pumping system which facilitates to maintain the evacuation of the spectrograph chamber to a very low pressure ($\sim 10^{-3}$ torr) while a pressure of 40 torr is maintained in the discharge tube.

We have designed and fabricated such a differential pumping arrangement and have photographed the helium emission continuum (110-600 Å). This continuum is now being used for absorption spectral investigation in this region.

References

1. P.G. Wilkinson and Y. Tanaka, J.Opt.Soc.Am. 45, 344 (1955)
2. Y. Tanaka, J.Opt.Soc.Am. 45, 710 (1955)
3. J.J. Hopfield, Phys.Rev. 35, 1133 (1930); 36, 784 (1930)
4. Y. Tanaka, A.S. Jursa and F.J. LeBlanc, J.Opt.Soc.Am. 48, 304 (May 1958).

5. Rydberg Transitions of S_2

(C.G. Mahajan*, G. Lakshminarayana and N.A. Narasimham)

The vacuum ultraviolet spectrum of S_2 is known to have three regions of absorption bands which belong to $C^3\Sigma_u^- \leftarrow X^3\Sigma_g^-$ (1) system (1850-1700 Å), $D^3\pi_u \leftarrow X^3\Sigma_g^-$ (2) system (1780-1650 Å) and E, F $\leftarrow X^3\Sigma_g^-$ (3) system (1550-1400 Å). The first and the last systems have been shown to belong to the first two members of the Rydberg series,

$$\ldots\ldots\ldots (\pi_g 3p)^2,\ ^3\Sigma_g^- \qquad (\pi_g 3p)(\pi_u np)$$

where n = 4 for state C

n = 5 for states E & F.

With a view to find the higher members of this Rydberg series we have investigated the absorption spectrum of S_2 in the 1600-1100 Å region.

The spectra were recorded by using the so-called "after-glow method. A mixture of sulphur vapour and purified helium or argon was subjected to r-f discharge in a side tube. (The r-f leads were so adjusted that the r-f discharge glow did not extend into the main absorption cell and this is why it is called the "after-glow" method). The discharge products from the side tube enter into the absorption cell and were being continuously pumped out. The absorption cell, 50 cm long and 2.5 cm dia. pyrex tube was placed between the spectrograph fluorite window and the krypton or argon continuum source. The spectra were recorded on a 3-meter normal incidence concave grating vacuum spectrograph (plate factor 5.6 Å/mm).

* DAE Junior Research Fellow

Kodak SWR and Ilford Q2 plates were used.

In the present work, besides the known absorption bands of S_2 in the vacuum ultraviolet region, many new absorption bands have been photographed in the region 1500-1380 Å. S_2 seems to be transparent in the region 1380-1200 Å as no absorption could be observed under various conditions. Photometric trace of the S_2 absorption bands in the 1520-1380 Å region is shown in the Figure 12.

(A) Rydberg series

$$\ldots\ (\pi_g 3p)^2,\ X^3\Sigma_g^- \qquad\qquad \ldots\ (\pi_g 3p),\ ^2\pi_g + (\pi_u np)$$

i) States E & F

E ← X and F ← X progressions, originally photographed by Donovan et al[3] were interpreted as the two spin states of S_2^+ core, viz, $^2\pi_{3/2}$ and $^2\pi_{\frac{1}{2}}$ having a separation of 400 cm^{-1}. As these states, like many excited states of O_2 [4] are approximating to (Λ, ω) coupling[5], each band should show the doublet structure. Because of the better resolution employed in the present work, each band could be seen to have a very clear doublet structure. In addition to this, one could easily see the degradation exhibited by some of the bands. The band head data of these two progressions are given in Table I.

ii) Progression IV

Progression IV has the intensity and vibrational quanta very similar to that of progression E ← X. The (0,0) band of the new progression is not observed, which is not unexpected as the ω_e value is increased from

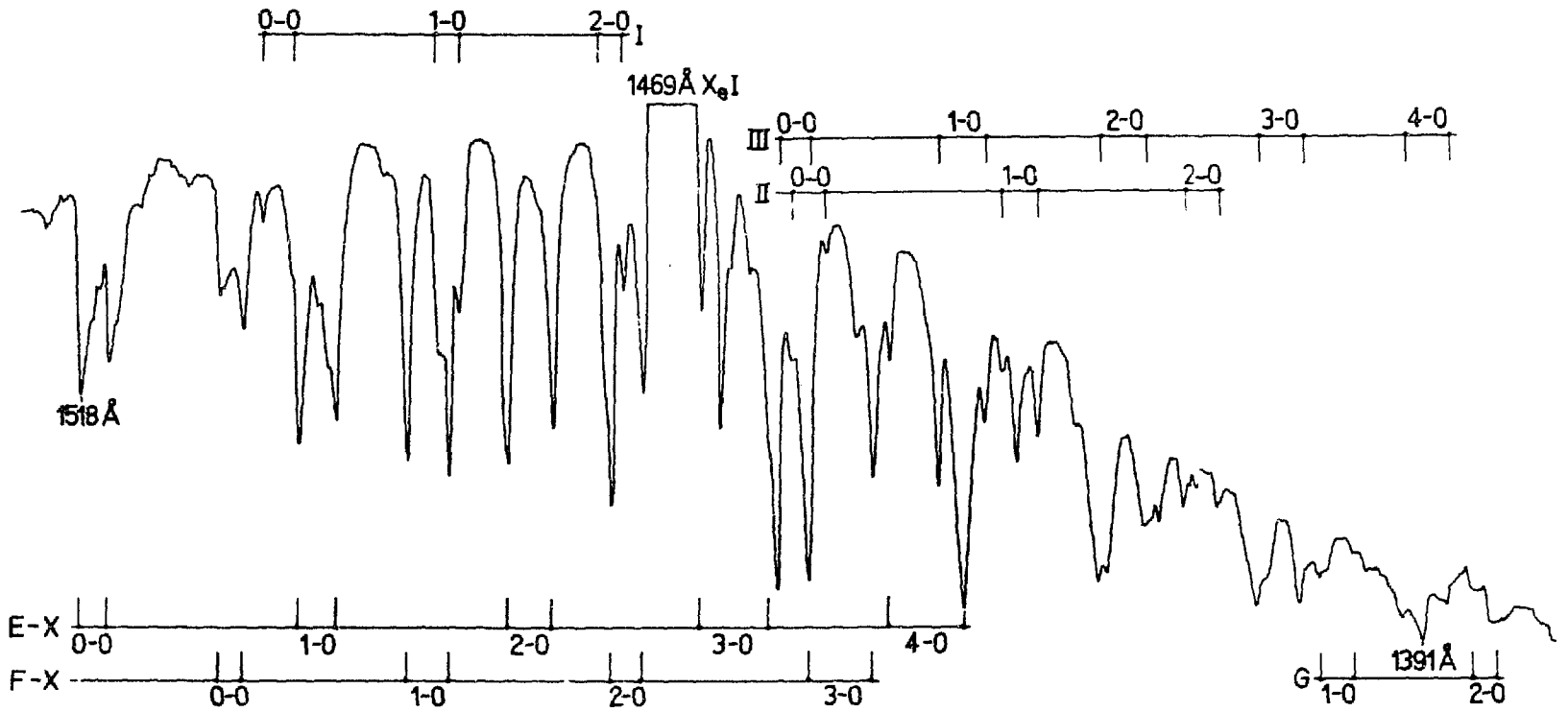

FIG. 12. VACUUM ULTRAVIOLET SPECTRUM OF S_2

725 cm^{-1} for ground state, $X^3\Sigma_g^-$ to 820 cm^{-1} for the excited state and hence the maximum intensity is shifted away from the (0,0) band. The band head data are given in Table II. Putting ν_{00} = 69925 cm^{-1}, the expected position of (0,0) band together with the atomic data in the Rydberg formula

$$\nu = I.P - \frac{R}{(n-\delta)^2} \quad \text{where } n = 6$$

δ, quantum defect = 1.67 (6)

We get a value of 9.39 eV for the first ionization potential of S_2 which is in close agreement with the value of 9.36 $\pm$ 0.02 eV obtained by Berkowitz(7) from the photoionization mass spectrometry.

Thus from all the above considerations, this new progression is, in all probabilities, the third member of the Rydberg series.

(B) Progressions I, II & III

Among the new bands photographed we have tentatively classified most of the bands into three different progressions. The band head data of these progressions are given in Table III. The intensities, growth and decay of these progressions are similar to that of B $\leftarrow$ X and F $\leftarrow$ X progressions of S_2. Thus the carrier of these progressions is also assumed to be sulphur molecule.

In addition to the above four progressions, there are some bands which could not be fitted in one or the other progression. Their wavelength an corresponding wavenumber values are given in the Table IV. Further analysis of these bands is in progress.

TABLE I

	E ← X			F ← X		
v',v''	λ in Å	ν cm^{-1}	Δ $G_{\frac{1}{2}}$ cm^{-1}*	λ in Å	ν cm^{-1}	Δ $G_{\frac{1}{2}}$ cm^{-1}*
0,0	1517.90	65876		1506.38	66280	
	1515.60	65980		1504.27	66384	
			818			827
1,0	1499.77	66676		1490.718	67081	
	1496.61	66817		1487.274	67237	
			789			755
2,0	1482.719	67443		1473.83	67850	
	1478.664	67628		1471.05	67978	
			788			818
3,0	1466.44	68192		1457.499	68610	
	1460.83	68454		1452.333	68854	
			746			780
4,0	1450.889	68923		1441.684	69363	
	1444.773	69215		1435.501	69662	

* Δ $G_{\frac{1}{2}}$ values are calculated after taking the mean of the doublets.

TABLE II

PROGRESSION IV

v,v''	λ in Å	ν cm^{-1}	Δ G 1/2 cm^{-1}*
0,0	-	-	
	-	-	
1,0	1415.359	70655	
	1411.693	70836	
			787
2,0	1400.283	71414	
	1395.689	71649	
			788
3,0	1385.60	72170	
	1379.90	72468	

* $\Delta G_{1/2}$ values are calculated after taking the mean of the doublets.

Table 1.

	Progression I			Progression II			Progression II		
v'v"	λ in Å	ν cm^{-1}	Δ $G_{\frac{1}{2}}$ cm^{-1}*	λ in Å	ν cm^{-1}	Δ $G_{\frac{1}{2}}$ cm^{-1}*	λ in Å	ν in cm^{-1}	Δ $G_{\frac{1}{2}}$ cm^{-1}*
0,0	1502.939	66536		1456.221	68670		1460.110	68487	
	1500.397	66649		1453.777	68786		1457.499	68610	
			538			740			659
1,0	1488.38	67186		1440.334	69428		1446.834	69116	
	1486.44	67274		1438.668	69508		1443.023	69298	
			627			695			643
2,0	1474.44	67822		1426.741	70089		1433.307	69768	
	1472.909	67892		1423.725	70238		1429.946	69932	
									630
3,0							1420.614	70392	
							1417.059	70568	
									603
4,0							1408.693	70987	
							1404.893	71179	

* Δ $G_{\frac{1}{2}}$ values are calculated after taking the mean of doublets.

TABLE IV

λ in Å	ν in cm^{-1}
1520.773	65756
1504.272	66477
1498.328	66741
1497.495	66778
1482.330	67461
1464.832	68267
1464.110	68300
1462.499	68376
1428.669	69995
1406.782	71084
1402.693	71291
1401.283	71363
1394.505	71710
1391.060	71885

References

1. R.F. Barrow and R.P. du Parcq, Elemental Sulphur, Ed. G.B. Meyer, (Interscience, New York, 1965).

   R.F. Barrow, R.P. du Parcq and J.M. Ricks, J.Phys. B., Series 2, 2, 413 (1969).

2. J.M. Ricks, R.F. Barrow, J.Phys. B., Series 2, 2, 906 (1969).

3. R.J. Donovan, D. Husain, and C.D. Stevenson, Trans. Fara. Soc. No.665, 66, Part I, (January 1970).

4. W.C. Price and George Collins, Phys. Rev. 48, 714 (1935).

5. R.S. Mulliken, J. Amer. Chem. Soc., 86, 3183 (1964).

6. Nat.Bur.Stand. Circ. 467 (Atomic Energy Levels), 1958.

7. J. Berkowitz and C. Lifschitz, J.Chem.Phys. 48, 4346 (1968).

---

6. Flash Photolysis of Methyl Formate

(S.L.N.G. Krishnamachari)

In continuation of the work on the flash photolysis of methyl formate, d-methyl formate and methyl formate-d_3, the flash photolysis of fully deuterated methyl formate ($DCOOCD_3$) has been completed. From these studies it is found that the methoxyl radicals (CH_3O) formed during the photodecomposition of the parent molecule are about four times as efficient as the formyl radicals (HCO) in producing formaldehyde.

7. Mercury Sensitised Photodecomposition of Organic Compounds

(S.L.N.G. Krishnamachari)

When hydrogen is photodecomposed in the presence of mercury vapour, the absorption spectrum of the HgH radical lying at 4000 Å could be seen. The HgH, evidently, has been formed as a result of the reaction of the excited mercury atom in the ^3P level with hydrogen molecule and the decomposition of the hydrogen molecule has taken place through the sensitised photodecomposition. Experiments are under way to determine the lifetime of these excited mercury atoms and also to examine the possibility of utilising the technique of sensitised photodecomposition to other organic molecules and observe the spectra of transient species.

8. Determination of the Structure of Polyatomic Molecules from Rotational Constants. S-Tetrazine.

(V.A. Job)

The complete structure of a polyatomic molecule can be determined from 3N-6 independent parameters where N is the number of atoms in the molecule. When the molecule has some symmetry and if the symmetry group of the molecule is known from other considerations, the number of parameters to be determined reduces to the number of totally symmetric vibrational modes. Even this number is usually much larger than the number of independent rotational constants.

A complete derivation of the structure is possible if we have the experimental data on sufficient number of isotopic species of the molecule.

We have written a computer program for the determination of the structure of a molecule by a least squares fit of the rotational constants of various isotopic species. The rotational constants can be given as any combination of I_A, I_B, I_C, A, B, C, $\bar{B}$ and K. The program was used for the determination of the structure of s-tetrazine in the ground ^1A_g state and excited $^1B_{3u}$ state.

The structure of s-tetrazine was derived by Merer and Innes[1] from the $\bar{B}$ values of six isotopic species of tetrazine, i.e., tetrazine-h_2, d_2, hd, $N_2^{15}h_2$, $N_2^{15}d_2$ and $N_2^{15}hd$, with certain approximations. Since then more accurate values of the rotational constants of tetrazine-h_2 have been reported by Innes et al[2]. We have tried to refine the structure by incorporating the new data in our least squares program and without using the approximations adopted by Merer and Innes.

It was found that a unique structure cannot be determined from $\bar{B}$ values alone. In order to determine a unique structure the K-value or separate values for two of the three rotational constants have to be given for atleast one of the isotopic species. The structures which give the best fit with the observed constants are given below:

	^1A_g	$^1B_{3u}$
r-CH	1.115 Å	1.056 Å
r-CN	1.330	1.387
r-NN	1.341	1.228
NCN	126.0°	117.1°

1. A.J. Merer and K.K. Innes, Proc.Roy.Soc. A302, 271 (1968).
2. Innes et al, J.Mol.Spectry. 40, 177 (1971); 43, 477 (1972).

9. Construction of a Nanosecond Flash Photolysis Unit

(S.L.N.G. Krishnamachari)

The introduction of lasers in the flash photolysis technique extends the resolvable time from the microsecond to the nanosecond range. For this purpose, a laser whose radiation is in the ultraviolet region is required to bring about the initial photodecomposition and another laser which serves as a source of continuous radiation and the appropriate delay mechanism are also required. Frequency doubling of the ruby laser radiation or a pulsed nitrogen laser which gives radiation in the ultraviolet region would serve as a convenient source for initiating the photodecomposition. The design of this set up is completed and the required components are being procured.

II(e). VIBRATIONAL SPECTRA AND MOLECULAR STRUCTURE

1. Calculation of Centrifugal Distortion Constants of Large Molecules

(R. D'Cunha)

A computer program has been written for the evaluation of the centrifugal distortion constants of substituted benzenes. Using the force constants obtained by Long and Steele[1], the centrifugal distortion constants for pentafluorobenzene (C_6F_5H) have been calculated and compared with those obtained from the microwave spectrum.

It was found that centrifugal distortion constants were not very sensitive to changes in the force constants.

1. D.A. Long and D. Steele, Spectrochim.Acta 19, 1947 (1963).

2. Normal Coordinate Analysis of CF_3 SeCl and CF_3 SeCN

(N.D. Patel and P.K. Wahi)

A normal coordinate analysis is being made for the molecules CF_3SeCl, CF_3SeBr and CF_3SeCN. Recently, one of us (P.K. Wahi)[1] has obtained infrared spectra of these molecules in gaseous state and Raman spectra in liquid state for these compounds. The kinetic energy matrices for these molecules have been computed using GMAT computer programme. A Modified Valence Force Field is proposed to be utilized for the calculation and the initial set of force constants are transferred from the trifluoro-

methyl compound, such as P $(CF_3)_3$ and some selenium halide.

3. Vibrational Spectra and Normal Coordinate Analysis of 4-Methyl and 5-Methyl Pyrimidines

(Y.A. Sarma)

Earlier, we have assigned the fundamental frequencies of pyrimidine, pyrimidine-d_4 and 2-chloropyrimidine, by doing a normal coordinate analysis[1]. To test the uniqueness of the set of potential energy constants thus obtained, we are extending these studies to 4-methyl and 5-methyl pyrimidines for which the vibrational spectra data is available. The initial results show satisfactory agreement between the observed and calculated frequencies. Refinement of force constants is in progress.

1. Y.A. Sarma (Spectrochim. Acta - in press).

4. Vibrational Spectra and Normal Coordinate Analysis of Benzotrifluoride

(V.B. Kartha and R. D'Cunha)

In continuation of the study of spectra of substituted benzenes[1,2], a detailed study of the infrared and Raman spectra of $C_6H_5CF_3$ and $C_6D_5CF_3$ has been carried out. Careful measurements, on purified samples, of band contours in the infrared and depolarisation ratios of Raman spectra have given unambiguous assignments for the CF_3 modes, F - CF_3 stretching mode and several in-plane and out-of-plane bending modes. Normal coordinate analysis incorporating these revised assignments has now been completed and

shows very good agreement between calculated and observed frequencies. As in the studies with other substituted benzenes[1,2], these quantitative calculations have shown very good correlation between the vibrational modes of benzene and substituted benzenes. Some of the redundancies overlooked in calculation by other authors[3] have also been included in the present studies.

1. N.D. Patel, V.B. Kartha and N.A. Narasimham, J.Mol.Spectry. 48, 185-201 (1973).
2. Ibid, pp.202-211 (1973).
3. C. LaLaw and R.G. Snyder, Spectrochim. Acta, 27A, 2073 (1971).

5. Vibrational Spectral Studies on Isotopic Borazines

(G.S. Ghodgaonkar and V.B. Kartha)

As discussed in earlier studies[1,2,3], the structural information as well as vibrational spectral data of this important boron ring compound is rather incomplete and we have undertaken a detailed study of the various isotopic borazines. Borazine and partially deuterated borazines have been synthesised and their infrared spectra have been obtained. In order to get information on structural parameters a high resolution spectral study is planned. The expected fine structure in rotational Raman spectra and vibration-rotation spectra have been calculated with an assumed D_{3h} structure. Experimental set up for obtaining such high resolution spectra is now being planned.

1. G.S. Ghodgaonkar and V.B. Kartha, B.A.R.C.-684, 100, (1973).
2. V.B. Kartha, S.L.N.G. Krishnamachari and C.R. Subramanian, J.Mol.Spectry., 23, 149 (1967).
3. V.B. Kartha and N.A. Narasimham, International Conference on Spectroscopy, Invited Talks, Bombay, January (1967).

6. Spectroscopic Studies on Rare Earth Complexes

(V.B. Kartha and T.S. Sugandhi)

Previous studies[1] on the spectra of rare earth formates have shown that the C-H frequencies in these formates are very sensitive to their coordination strength. In order to correlate the two quantities more accurately, a detailed study of the infrared and Raman spectra of rare earth formates have been undertaken. Raman spectra (and also laser induced fluorescence spectra) of several formates have now been obtained on the Spex 1401 Raman Spectrometer using 4416 Å excitation of a He-Cd laser at 15 MW power. The Raman studies have confirmed the results from infrared data. Further studies on the complete interpretation of the spectra is being carried out.

1. V.B. Kartha and N.V. Thakur, Proc. Chemistry Symp. Vol.II, 165-167 (1972), Aligarh Muslim University, Dec. 21-23 (1972).

III. OPTICS

III(a) DESIGN AND FABRICATION OF OPTICAL COMPONENTS

1. Czerny Principle in Monochromator Design

(M.V.R.K. Murty)

Introduction

Recently, several authors[1-5] pointed out the existence of multiply dispersed light in existing commercial monochromators of Czerny-Turner type. Some of the early references to the multiply dispersed light may be found in the papers by Stamm and Salamon[6] and by Alpert[7]. The reason for this has been realised to be mainly due to the fact that the off-axis angle of the concave spherical mirrors is not large enough. In very high resolution type of instruments, the off-axis angle is invariably kept small to keep the contribution of uncompensated coma and other aberrations as low as possible. In these instruments the problem of multiply dispersed light is sometimes very serious and the theory of this phenomenon has been presented by Mitteldorf and Landon[8] and also by Pribram and Penchina[9]. Multiply dispersed light is not present for all positions of the diffraction grating but only in certain regions as discussed in refs. (8) and (9). We shall not go into the above details for the prediction of multiply dispersed light here. Recently, Hill[10] and also Chupp and Grantz[11] have proposed to convert the spherical mirrors of the conventional Czerny-Turner monochromator into off-axis paraboloids thereby increasing

the off-axis angles on the mirrors to such a large value that the problem of multiply dispersed light does not arise. However, the coma cancellation along the length of the slit requires that the U- configuration rather than Z- configuration be used for the monochromator[11]. Hawes[12] and also Chupp and Grantz[11] point out a principle, attributed to Cary, which enables the determination of the minimum off-axis angle required in any in-plane monochromator design so that multiply dispersed light cannot occur. This principle is very elegant and simple to use. We shall see how this principle can be used to devise a Czerny-Turner monochromator design in which the off-axis angles of the spherical mirrors are kept very small.

Cary Principle

Cary principle may be stated in the following way: Arrange the collimator mirror and focussing mirror in such a way that the normals to the inner edges of these mirrors will not pass through the aperture of the dispersing element. Thus for a given relative position of the spherical mirror and the plane diffraction grating, there is a particular minimum off-axis angle which should be used to avoid multiply dispersed light. Fig. 1 indicates the geometry of such a situation from which we can derive the following relationship:

$$f^{*} \quad \theta \quad > \quad (4-K) \quad /2 \quad K \qquad \text{----------} \qquad (1)$$

Where f^{*} = F- number of the instrument in the plane of dispersion,

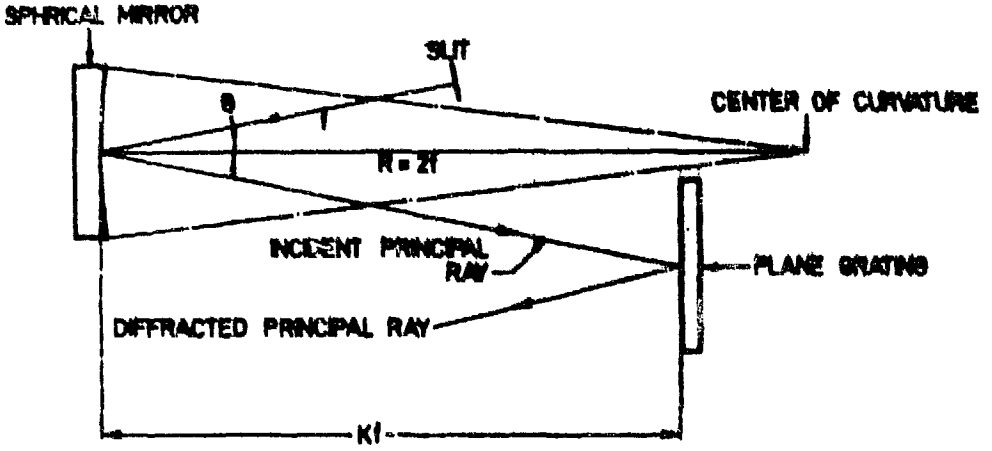
SPHRICAL MIRROR
SLIT
CENTER OF CURVATURE
R = 2f
INCIDENT PRINCIPAL RAY
PLANE GRATING
DIFFRACTED PRINCIPAL RAY
Kf

FIG. 13.

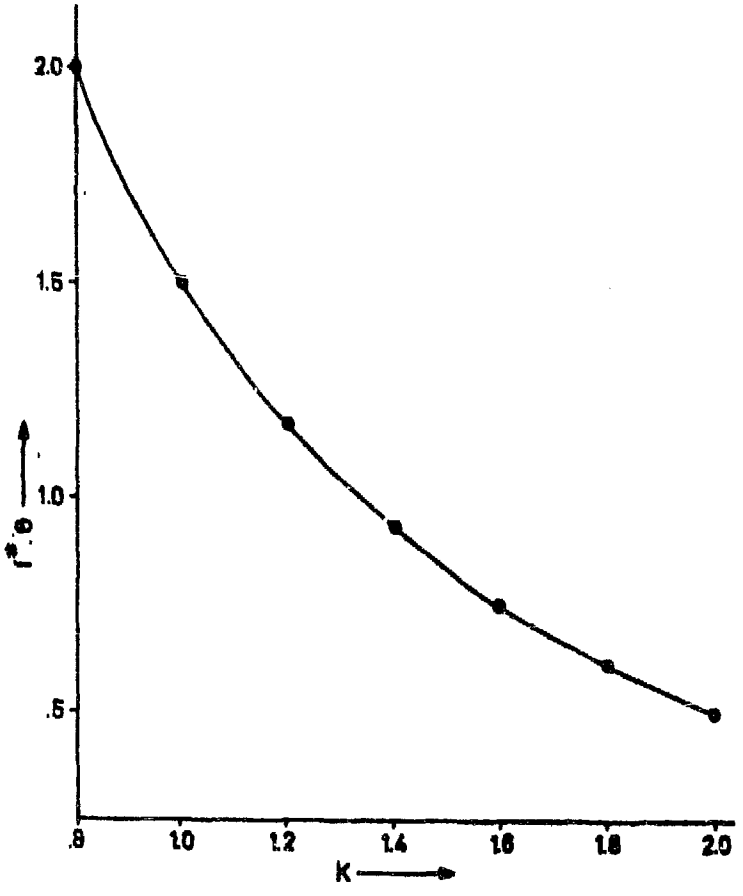
2.0
1.5
1.0
.5
r*.e
.8
1.0
1.2
1.4
1.6
1.8
2.0
K

FIG. 14.

θ = off-axis angle of the concave mirror as indicated in Fig.1,

and K = factor indicating the position of the plane grating relative to the concave mirror.

Thus Kf is the distance of the plane grating from the spherical mirror of focal length f.

The above relation reduces to:

$$f^{\#} \quad \theta \; > \; 1.5 \qquad \text{----------} \qquad (2)$$

given by Chupp and Grantz[11] when K = 1. Fig.14 shows a plot of $f^{\#}$ θ vs. K where the range of values chosen for K is from 0.8 to 2.0. The value of K = 0.8 corresponds to roughly the position chosen for the plane grating in the commercial monochromators. It is seen easily from Fig.2 that the minimum permissible off-axis angle comes steeply down for a given $f^{\#}$ as K increases to 2.0. The value of $f^{\#}$ θ is 2.0 for K = 0.8 while it is only 0.5 when K = 2.0. Thus there is a 4-fold reduction in the value of minimum off-axis angle. The value of K = 2.0 corresponds to the position of the plane grating being located by the side of the centre of curvature of the spherical mirror. There is no special advantage to go beyond the value of K = 2.0.

Monochromator

Utilising the above principle, we may now see what is the physical arrangement for a monochromator using a nominal 100 x 100 mm plane grating and a nominal focal length of 750 mm. Using the value of K = .85 and $f^{\#}$ = 7.5 the minimum off-axis angle θ to avoid multiply diffracted light is 14.2°. However, the off-axis angle used in a

commercial instrument with the above parameters is only 6.75°. Of course, ...s is done to keep down the off-axis aberrations and maintain a higher ...olution. Now let us see what is the minimum off-axis angle when K = 2.0. This turns out to be 3.82°. Thus the requirement on the minimum off-axis angle has been drastically cut down when K = 2.0.

Of course, in this design the entrance and exit slits are somewhat awkwardly situated and also the physical length of the instrument is increased. Also, to clear the positions of the entrance and exit slits from the collimated beams, one should actually use off-axis angles slightly larger than the calculated ones from the relation (1). A schematic diagram of a monochromator is shown in Fig.15 based on the principles enunciated above. One may be inclined to frown upon such a design since the instrument is much larger than the conventional Czerny-Turner monochromator. But one should remember that people are putting up with Schmidt cameras which are two times as long as their focal lengths. In fact, the proposed design of the monochromator has the resemblance to the Schmidt system in so far as the plane grating (aperture stop) is located at the plane of centres of curvature. The two centres of curvature of the collimating and focussing spherical mirrors lie on either side of the dispersing element as though they are guards not letting any of the normals from the spherical mirrors hit the dispersing element thus carrying the Cary principle to its logical conclusion. The above procedure is recommended only when the highest possible resolving power from an instrument with spherical mirrors is to be obtained without

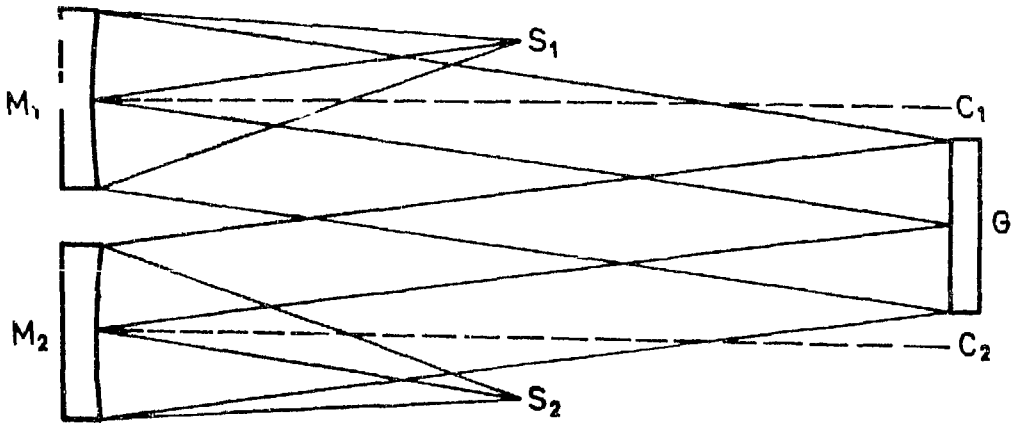

FIG.15.

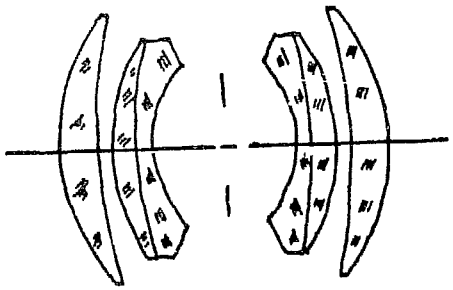

BIOTAR LENS

FIG.16.

the multiply dispersed light. Where such requirement is not needed as for instance in some illumination monochromators or monochromators used in some spectrophotometers of low resolution, the conventional value for K of about 0.8 should be chosen and the corresponding off-axis angle used for the mirrors. Actually, it is only necessary to choose for K a value of about 1.5 to 1.6 (not K = 2.0) and obtain reasonably small off-axis angles. It is probably necessary to use small plane mirrors near the slits to deviate the light by 90°. Thus in practice the instrument will be only 50 - 60% longer than the conventional monochromator.

References

1. A. Watanabe and G.C. Tabisz, Appl.Opt. 6, 1132 (1967).
2. C.M. Penchina, Appl.Opt. 6, 1029 (1967).
3. J.E. Tyler and R.C. Smith, J.Opt.Soc.Am. 56, 1390 (1966).
4. A.B. Shafer and D.O. Landon, Appl.Opt. 8, 1063 (1969).
5. A. Watanabe, Applied Spectroscopy, 22, 198 (1968).
6. R.F. Stamm and C.F. Salzman, Jr., Opt.Soc.Am., 43, 126 (1953).
7. N.L. Alpert, Appl.Opt. 1, 437 (1962).
8. J.J. Mitterldorf and D.O. Landon, Appl.Opt. 7, 1431 (1968).
9. J.K. Prijram and C.M. Penchina, Appl.Opt. 7, 2055 (1968).
10. R.A. Hill, Appl.Opt. 8, 575 (1969).
11. V.L. Chupp and P.C. Grants, Appl.Opt. 8, 925 (1969).
12. R.C. Hawes, Appl.Opt. 8, 1963 (1969).

Figure No.	Title
13	Schematic diagram indicating the position of the plane grating in relation to the spherical mirror for deriving the relation for minimum off-axis angle θ in terms of f and the K-factor. Kf is the distance of the plane grating from the spherical mirror whose focal length is f and its f-N° is f .
14	Plot of f θ vs K.
15	Schematic diagram of the proposed monochromator in which very small off-axis angles can be used for the spherical mirrors and still the multiply dispersed light is kept out. M_1 and M_2 - Spherical mirrors; C_1 and C_2 - Centres of curvature of the mirrors; G-plane grating; S_1 and S_2 - The slits. The off-axis angles are not to scale. It is possible to choose a value K = 1.5 to 1.6 to obtain a more compact arrangement in practice. At the positions of the slits, two plane mirrors at 45° may be used for convenience (not shown in figure).

2. Design of a Double Gauss (Biotar) Lens System

(M.V.R.K. Murty and N.C. Das)

This type of lens consists of two divergent meniscus doublets concave towards a central stop and two outer convergent components. It is generally designed to cover a total field of 20° - 40° in focal lengths 1" - 6". It is possible to obtain a speed of f/1.5 for smaller field. For moderate and large fields speeds are generally f/2.5 and f/5.6 respectively. These lenses are generally used as photographic objectives and projection lenses and have got excellent image quality near the central portion of the field. The image quality gradually falls towards the outer portion of the field. Using India-made optical glasses we have designed a lens suitable for use in an overhead projector with the following specifications and design data. (Fig.16).

Focal length 14", speed f/4.5, plate size 10" x 10" and magnification 5X.

Radius	Thickness	Glass Type
133.2		
	21.0	DBC 610573
448.4		
	2.0	AIR
114.2		
	21.0	DBC 613568
302.8		
	8.4	DF 605380
68.9		
	54.9	AIR
- 76.6		
	9.45	DF 605380
- 578.2		
	21.0	DBC 610573
- 116.7		
	2.0	AIR
- 444.9		
	21.0	DBC 613568
- 122.4		

(Dimensions are in mm)

3. 12 x 50 Telescope Fabricated for Use in the Radiometallurgy Laboratory.

(M.V.R.K. Murty and A.L. Narasimham)

Porro prism system (first type) is always utilised in the telescopes required for general terrestrial usage and also for telescopes fitted in binoculars. But design of a still more compact telescope is possible by utilising a porror prism system (second type). Figure 17 shows how erection of an inverted image is achieved. In this system it is possible to replace by plane mirrors (ref. Fig.18) the right angled prisms which were used earlier for folding the light path by total internal reflections. Figs. 19(a) and 19(b) indicate the usage of right angle prisms for folding the path of light beam through 90°.

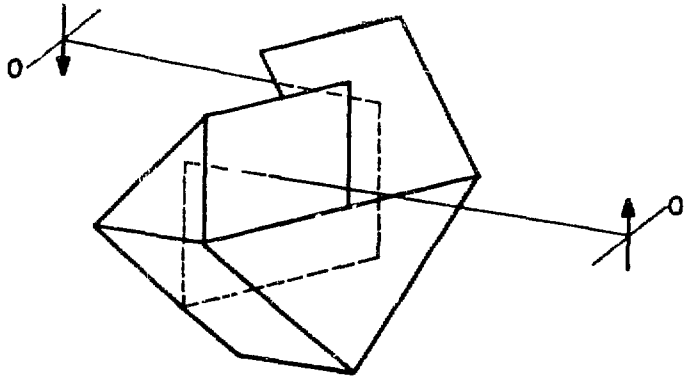

FIG. 17. PORRO PRISM SYSTEM (SECOND TYPE)

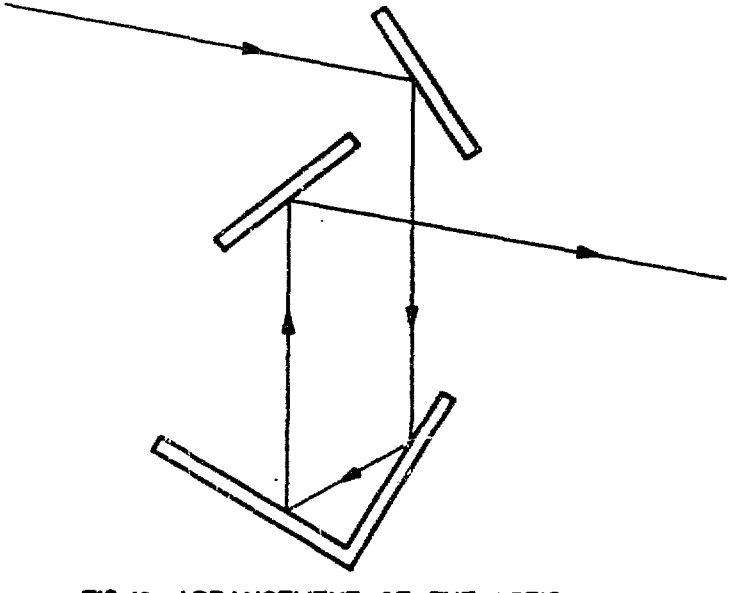

FIG. 18. ARRANGEMENT OF THE OPTICAL SYSTEM OF MIRRORS.

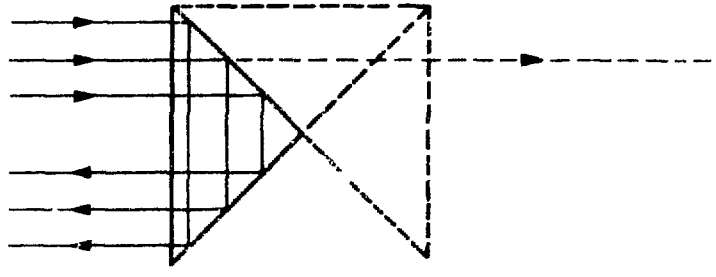

FIG. 19a. RIGHT ANGLE PRISM USED WITH HYPOTENUSE AS ENTRANCE AND EXIT FACE

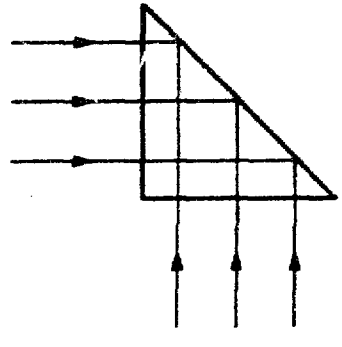

FIG. 19b. RIGHT ANGLE PRISM USED WITH HYPOTENUSE AS THE REFLECTING FACE

4. Direct Vision Spectroscope Utilising a Prism and a Transmission Grating of 600 grooves per mm.

(M.V.R.K. Murty and A.L. Narasimham)

This instrument has the merit of linear dispersion of radiations having different wavelengths, compared to non-linear dispersion of the instrument incorporating a single piece dispersion prism.

A grating of 600 lines per mm is chosen as the best since there is an upper limit to the practical number of grooves per mm for transmission gratings. This arises from the fact that as the angle of diffraction approaches the face angle of the groove, more and more of the light is lost by internal reflection.

Using for the grating a resin with index of refraction of 1.566, the critical angle is 39° 42'. Thus the maximum possible blaze angle for a transmission grating using such a resin is about 38°, at normal incidence.

From Fig. 20, $\frac{\text{Sin } \gamma'}{\text{Sin } 38^\circ} = 1.566$

Therefore $\gamma' = 74^\circ\ 38'$

and $\delta = 74^\circ\ 38' - 38^\circ$

$= 36^\circ\ 38'$

$d \text{ Sin } \delta = n \lambda$

Therefore $\text{Sin } 36'\ 38' = \frac{n \lambda}{d}$

where d is the groove spacing of the grating and n is the order of the

spectrum. For the first order

$$d = \frac{6500 \times 10^{-7}}{\sin 36° 38'} = \frac{6500 \times 10^{-7}}{0.5967}$$

taking $\lambda = 6500 \times 10^{-7}$ mm.

From this it follows that 900 grooves per mm is the practical upper limit for transmission gratings in visible light. To effect a compromise between (i) light losses by internal reflection, and (i') achieving adequate dispersion, a grating of 600 grooves per mm is chosen.

Radiation of wavelength 5500 Å gets diffracted through 19° 16'. By inserting a prism of suitable angle after the grating, this radiation is made to emerge in the same direction as the incident beam. If the angle of the prism is A and the index of refraction is 1.55,

$$\frac{\sin A}{\sin (A + 19° 16'} = \frac{1}{1.55}$$

Therefore A = 28° 34'.

By placing a prism of this angle against the grating the deviation in the beam as a result of passage through the grating will be annulled but the dispersion of the grating is slightly enhanced by an amount nearly equal to the dispersion of the prism. This is shown in Fig.21.

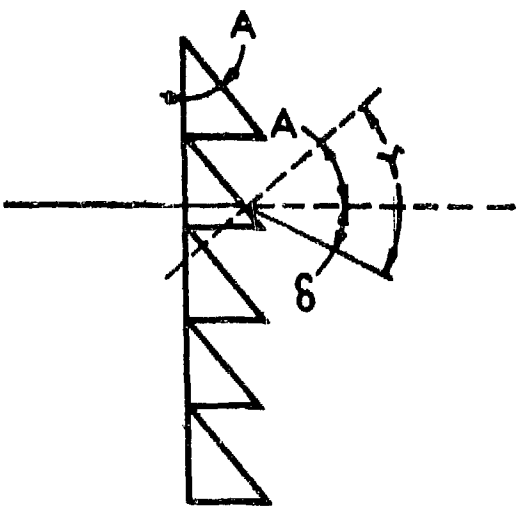
A
A
δ

FIG. 20.

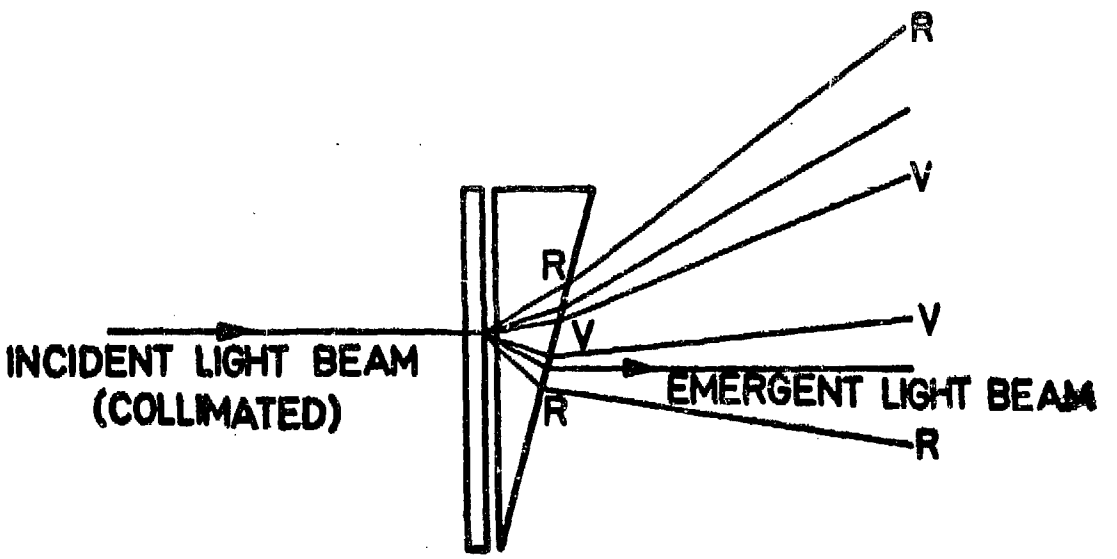
R
V
R
V
V
INCIDENT LIGHT BEAM
(COLLIMATED)
EMERGENT LIGHT BEAM
R
R

FIG. 21.

III(b) INTERFEROMETRY

1. Jamin Interferometer Using a Laser Source

(M.V.R.K. Murty and R.P. Shukla)

The conventional Jamin interferometer consists of two identical parallel plates of glass. It is generally used with an extended source of white light. The instrument has been found to be extremely useful by using a collimated beam of light. When the collimated beam is obtained from a white light source it is necessary to obtain complete compensation in both beams. This version was used earlier for determining extremely small differences in refractive indices of two liquids. The present version is used with collimated light from a laser source and it is found to be useful for testing parallelism of windows and other optical elements. A high quality collimating lens is required for this instrument. To increase the versatility of the instrument a double wedge arrangement is used in one of the beams so that a background of straight fringes with variable separation and direction can be obtained. A typical schematic diagram of the instrument is shown in Fig.22.

This interferometer is extremely useful in various fields of research such as aerodynamics, diffusion studies, heat transfer studies etc. in addition to optical testing of optical components.

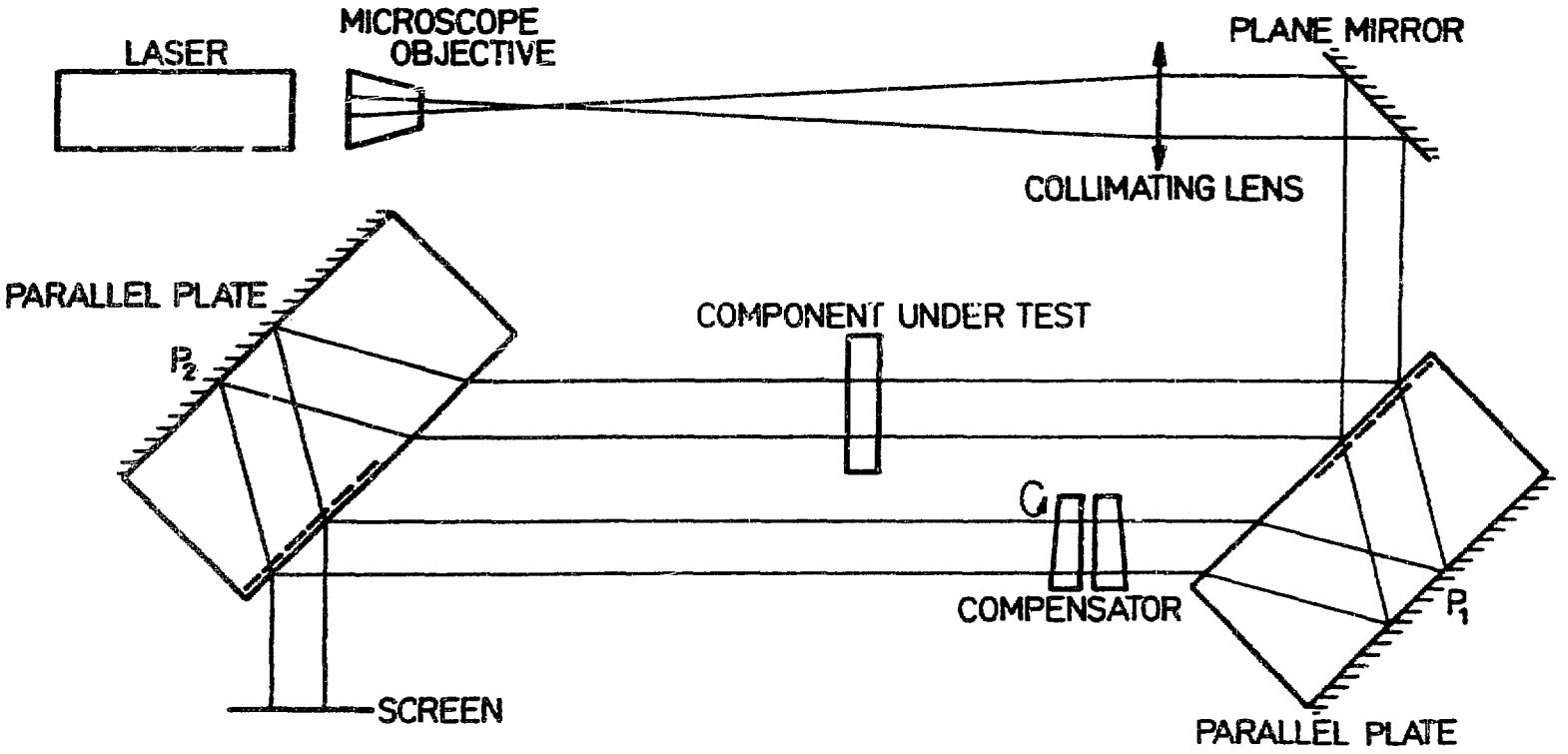

FIG.22. SCHEMATIC DIAGRAM SHOWING THE JAMIN INTERFEROMETER USING A LASER SOURCE

III(c) THIN FILMS

1. Equipment for the Fabrication of Multilayer Optical Thin Film Devices.

(K.V.S.R. Apparao)

Multilayer optical thin film devices such as Fabry-Perot mirrors, laser mirrors, interference filters etc. are made by depositing in vacuum a number of thin films of different dielectric materials of specified thicknesses one over the other on a suitable substrate plate. Each film in such a stack should be very uniform and to fabricate such spectrally good quality thin film devices a big coating plant of atleast 19" chamber diameter and a good optical film thickness monitor are necessary.

A vacuum coating plant of 19" chamber with different accessories is designed and will be fabricated in the division. Some major parts for this unit are ready for assembly and some more accessories for this unit are designed and the detailed working drawings for the following parts are made: 1) Beam guide light tube for thickness monitor; 2) Rotating substrate holder; 3) Baffle plate with shutter assembly; 4) Valve base plates; 5) Substrate heater; 6) Gauge adopter, and 7) Multifilament turret.

For monitoring the thickness of thin films accurately during deposition an optical monitor is designed and the optical set up of this unit is fabricated, fitted and aligned to the existing 12" vacuum coating plant. This assembly generates a modulated light beam and a guide tube

takes this beam from outside through a substrate in the vacuum chamber and leads the beam out of the chamber to a photomultiplier. The electronics part of this unit is fabricated and is being tested for its optimum performance.

2. An Improved Optimization Method of Designing Thin Film Filters

(K.V.S.R. Apparao)

The problem of designing a practically realisable multilayer filter to meet the given optical specifications is often a difficult task because of the complex calculations involved in solving the problem. Methods of automatic synthesis of filter design using digital computers have not so far proved completely successful. An alternate approach which is more encouraging is to solve the problem by optimization (refining) methods. Method of damped least squares is applied for the first time to the present problem of designing thin film filters.

According to the present method, any filter can be designed to the given optical specifications in three independent stages. In the first stage an initial simple design whose transmittance characteristic matches very approximately with the desired characteristic is chosen and this initial design is improved using matching techniques in the second stage by changing thicknesses of certain films. In the final stage called optimization method, the design is further improved by changing the thicknesses of some more layers. Optimisation method consists of

calculating the partial derivatives of the reflectance of the filter with respect to the individual film thicknesses at each wavelength and ...ving for the thickness increments which provide a better fit. These new thickness increments are incorporated in the initial design and the performance of the improved design is obtained. The calculations are repeated, taking the above design as a starting point, in an iterative way until the required optical specifications of the filter are obtained.

The present improved optimization method is developed using BESM-6 computer and is being applied successfully for designing edge filters. Fig.23 illustrates the principle of the present method of design and the results for an edge filter design. Curve A shows the transmittance of an initial simple 17 layer, of alternate low and high index films, quarter wave stack wherein the ripple in the pass band which cannot be tolerated for an edge filter is present. But for the improved design B which is obtained after matching techniques the ripple in the pass band is reduced to a certain extent whereas for the final design C obtained after optimisation the ripple in the pass band is reduced to a certain extent and also the edge became more straight which are the main requirements for an edge filter. Work on certain improvements in the method for designing other types of filters is in progress.

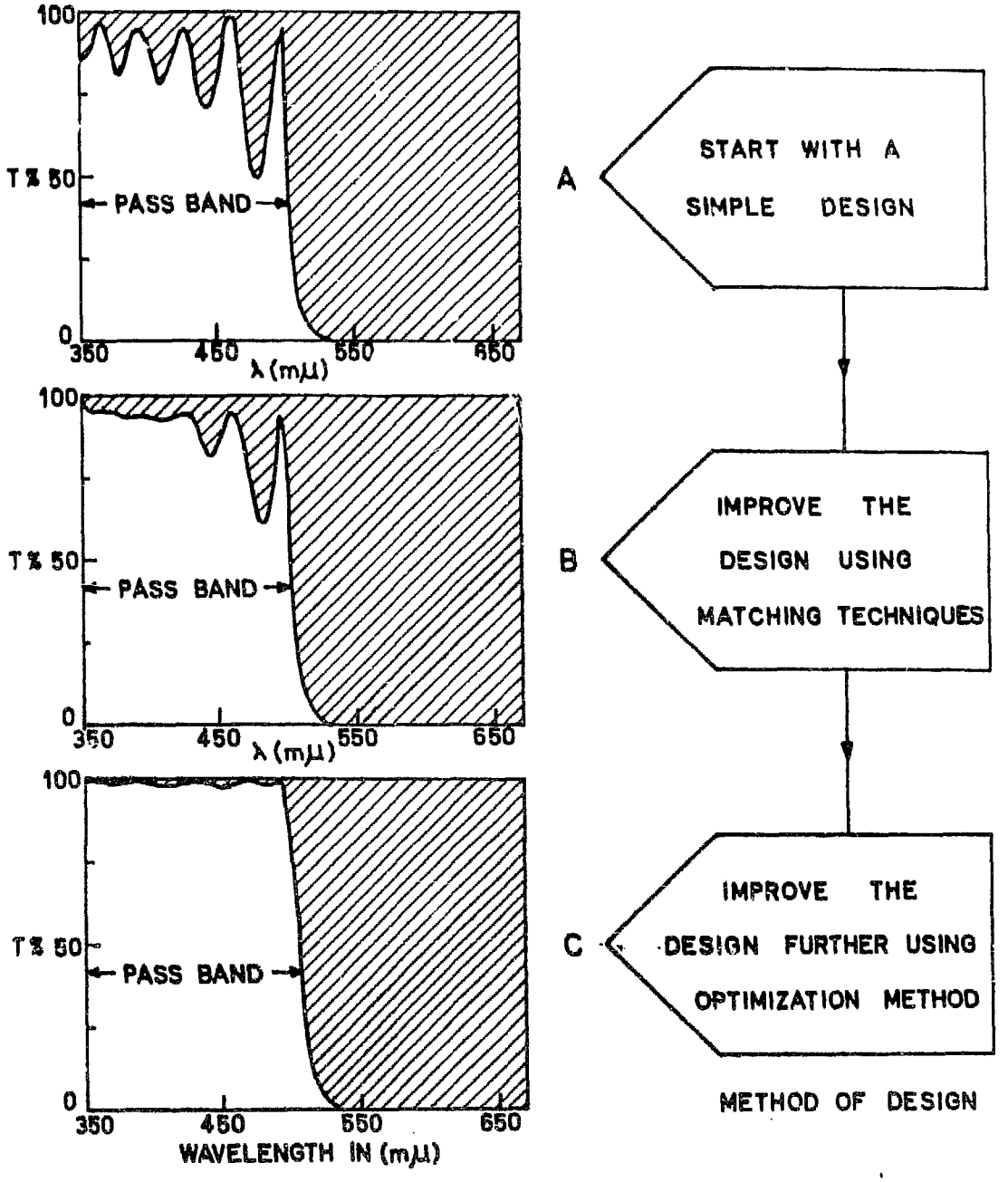

FIG.23. PRINCIPLE OF THE METHOD OF DESIGN & THE TRANSMITTANCE OF THE EDGE FILTER DESIGNS DESCRIBED IN TABLE I.
(A: INITIAL DESIGN, B: IMPROVED DESIGN, C: FINAL DESIGN)

TABLE I

Optical Description of the Edge Filter Designs shown in Fig.1

Layer	Index	Wavelength in mμ at which the layer is quarterwave thick		
		Initial starting Design A	Improved Design B	Final Design C
	1.0	Massive	Massive	Massive
1	1.38	600.0	300.0	325.0
2	2.30	600.0	600.0	630.0
3	1.38	600.0	600.0	619.0
4	2.30	600.0	600.0	611.0
5	1.38	600.0	600.0	613.0
6	2.30	600.0	600.0	598.0
7	1.38	600.0	600.0	590.0
8	2.30	600.0	600.0	591.0
9	1.38	600.0	600.0	594.0
10	2.30	600.0	600.0	594.0
11	1.38	600.0	600.0	593.0
12	2.30	600.0	600.0	596.0
13	1.38	600.0	600.0	604.0
14	2.30	600.0	600.0	615.0
15	1.38	600.0	600.0	629.0
16	2.30	600.0	600.0	670.0
17	1.38	600.0	300.0	780.0
	1.52	Massive	Massive	Massive

(n_L = 1.38 - MgF_2 ; n_H = 2.30 - ZnS)

3. Thin Film Reflectometer
(K.V.S.R. Apparao)

The development of complex systems of multilayer dielectric thin film devices brings with it a requirement for precise measurement of spectral reflectances of plane specular surfaces. Most existing reflectometers suffer from either or both of two major faults - reflectometers are mostly measured with the incident beam at an appreciable angle to the normal, and many methods give comparative rather than absolute reflectance values, necessitating a reference surface to convert the former to the latter.

A reflectometer is designed to measure the absolute reflectance of dielectric filters and is being fabricated in the division. Fig.24 shows schematically the principle of the reflectometer. Light from the exit slit S_1 of the monochromator is converged in a cone of small angle (less than 1°) by a lens L and falls on the sample X at normal incidence. Part of the incident flux is transmitted and part reflected. Two identical semi-reflecting mirrors M_1 and M_2 equally inclined at an angle of about 40° to the incident beam direct equal amounts of the reflected and transmitted beams to form images of S_1 at a detector D. The detector should be of such nature and so positioned as to give equal sensitivity for each direction M_1 D and M_2 D and this can be achieved by using a diffuser before the photomultiplier. S_2 is a shutter to interrupt either beam M_1D or M_2D.

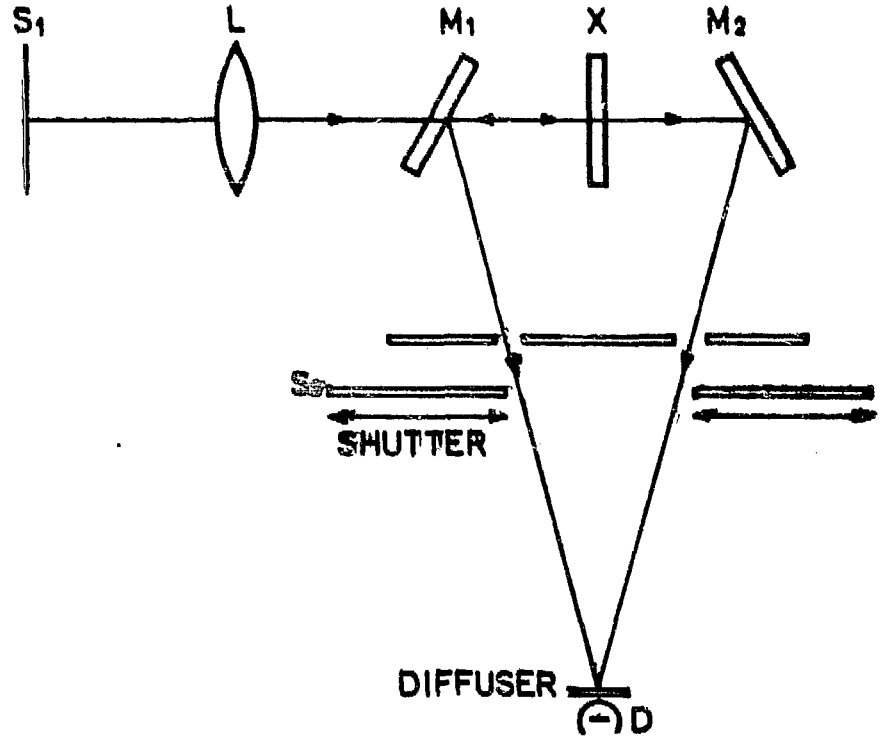

SCHEMATIC DIAGRAM OF THIN FILM REFLECTOMETER

FIG. 24.

Suppose that the reflectance of the mirrors M_1 and M_2 for the set angle of incidence, state of polarization and wavelength of the incident flux is r. Then for the sample X of absolute reflectance R and transmittance T with incidence flux F_o, the flux arriving at D via M_1 is

$$F_R = r.R.F_o$$

and the flux arriving at D via M_2 is similarly

$$F_T = r.T.F_o$$

with the sample removed, the flux arriving at D via M_2 is

$$F_1 = r.F_o$$

Hence $$R = \frac{F_R}{F_1}$$

and $$T = \frac{F_T}{F_1}$$

All the parts of this reflectometer are designed and are being fabricated in the division.

IV. SERVICE ELECTRONICS

The service electronics group, in addition to doing the regular maintenance of all electronic equipments in the division, also carries out the fabrication of the electronic instruments required by the various groups.

During this period, one signal amplifier, reference amplifier and a phase sensitive rectifier for the infrared isotopic analyser have been fabricated. The voltage gain of the signal amplifier is 2500. The noise referred to the input is 35 micro volts. Further tests on the linearity, stability etc. are in progress.

Two Zener stabilised power supplies capable of giving 25 mA at 4.5 d.c. with 1 MV P.P.ripple for Jacophones have been fabricated.

One higher voltage d.c. power supply capable of giving 5 to 15 mA around 3600 V d.c. to excite He-Ne laser has been fabricated. It gives an open circuit voltage of 6800 V d.c. for the initiation of the discharge.

Maintenance and servicing of all the existing electronic equipments in the division have also been done throughout the year.

APPENDIX I

PARTICIPATION IN SYMPOSIA, CONFERENCES AND SUMMER SCHOOLS

1. A review of the R & D activities of the division was held in January 1974 in which senior scientists of the division presented the Research and Development work being carried out in their respective fields.

2. Dr. N.A. Narasimham delivered a series of lectures at the Marathawada University, Aurangabad.

3. Dr. V.B. Kartha attended the "Workshop on Spectrophotometry", Indian Chemical Society, Bombay Branch, December 1973, and gave a talk on 'Basic Principles of Absorption Spectrophotometry'.

4. Dr. V.B. Kartha gave two lectures on Raman Scattering and Motion of Molecules in Condensed Systems, to the participants in the Course on 'Lasers and Light Scattering', Nuclear Physics Division, BARC, July 1973.

5. Dr. V.A. Job gave a seminar to the Chemical Physics Group at the Tata Institute of Fundamental Research, (October '73) on 'High Resolution Electronic Spectra of Polyatomic Molecules'.

6. Dr. P. Ramakoteswara Rao gave one lecture on "Communication with Extra Terristral Civilization" at the 'Antiobsolence Lectures-XXXX', September 1973.

7. Dr. R.C. Naik and Shri K.H. Ayyar presented a paper entitled "Absorption and Fluorescence Spectra of Europium and Terbium Trichloro-acetates" in the Symposium on Quantum and Opto-Electronics, February 1974.

Deputation

.. Dr. M.V.R.K. Murty went on deputation to Institute Nacional de ;trophisica Optica Y Electronica (INAOE), Mexico, as a Visiting Professor for a period of 4 months, from 4.2.73 to 5.6.73 and to the University of Rochester for a period of 2½ months from 5.10.73 to 14.12.73.

2. Dr. Mahavir Singh, who was on deputation to Belgium for training under the Indo-Belgium Nuclear Co-operation Programme for 1972-73, returned to India in May 1974.

APPENDIX II

POST-GRADUATE TEACHING, RESEARCH AND TRAINING TO OUTSIDE PERSONNEL

Dr. M.A. Narasimham and Dr. S.L.N.G. Krishnamachari taught the special subject Spectroscopy, comprising of papers V and VI of the M.Sc. (Physics) degree course of the Bombay University.

Dr. V.B. Kartha gave a course of lectures in Infrared and Raman spectroscopy to the Refresher School in Chemistry for University lecturers held by BARC.

Senior staff members of the division took part in the selection of candidates to the BARC Training School. They also gave lectures to the 17th course trainees.

The following scientists continue to carry out research work for M.Sc/Ph.D degrees:

Sl.No.	Name	Subject	Degree	University	Guide
1.	Shri S.V. Grampurohit	Phys.	Ph.D	Bombay	Dr. M.A. Narasimham
2.	" L.C. Chandola	"	"	"	"
3.	" S.A. Ahmad	"	"	"	"
4.	Smt. P.Meenakshi Rajarao	"	"	"	"
5.	Shri T.R. Saranathan	"	"	"	"
6.	" C.G. Mahajan*	"	"	"	"
7.	" T.V. Venkitachalam	"	"	"	Dr. S.L.N.G.K. Chari
8.	" M.D. Saksena	"	M.Sc.	"	"
9.	Kum. M. Saraswathy	"	"	"	"
10.	" Annamma Joseph	"	"	"	"
11.	Shri I.J. Machado	"	"	"	Dr. G.D. Saksena
12.	" A. Venugopal	"	"	"	"
13.	" P.P. Khanna	"	"	"	"
14.	" R.V. Subramanian	Chem.	"	"	Dr. V.B. Kartha
15.	" V.N.P. Kaimal	"	"	"	"
16.	" O. Thomas	"	"	"	"
17.	Kum. T.S. Sugandhi	"	"	"	"

* DAE Fellow

Thesis submitted:

Name	Degree	University	Guide
Shri G.L. Bhale	Ph.D.	Bombay	Dr. N.A. Narasimham

Title: "On the Second Negative Band System of $^{16}O_2^+$ and $(^{16}O^{18}O)^+$ "

Training

Sl.No.	Name of the scientist and institution.	Field of training	Duration
1.	Shri M.R. Belsare, Sri G.S.Institute of Technology & Science, Indore-3.	Spectrographic analysis of minerals and ores.	28.5.73 to 12.7.73
2.	Shri V.Panchapakesan, Indian Institute of Technology, Bombay.	-do-	12.6.73 to 12.7.73
3.	Shri N.N. Saxena, Holkar Science College, Indore.	Microphotometry	21.7.73 to 14.8.73
4.	Shri J.M. Quarbani, Faculty of Science, Kabul University, Afghanistan.	Spectrochemical Analysis and X-ray Fluorescence Analysis (Under Colombo Plan).	8.9.73 to 17.11.73
5.	Shri G.K. Bhatt, PRL, Ahmedabad.	Atomic absorption spectrophotometry and emission spectroscopy of metal samples.	15.10.73 to 15.12.73
6.	Shri J.M. Halam, & Shri B. Leelakrishnan, Hindustan Photo Films Mfg.Co.Ltd, Ootacamund	Spectrochemical Analysis	18.3.74 to 3.4.74

APPENDIX III

LIST OF PAPERS PUBLISHED IN JOURNALS/SUBMITTED FOR PUBLICATION

Sl.No.	Title of the Paper	Author/s	Journal
1.	A Carrier Distillation Method for the Analysis of Yttrium Oxide for Non-Rare Earth Impurities.	R.C. Naik and P.D. Karnik	Z.Anal.Chem. 265, 349 (1973).
2.	Intermittent A.C. Arc Method for Spectrographic Analysis of Tantalum Oxide.	L.C. Chandola and R.V. Subramanian.	Z.Anal.Chem. 266, 127 (1973).
3.	Sharpening the Fringes in the Ronchi Test.	M.V.R.K. Murty and A. Cornejo	App.Opt., Vol.12, No.10 (73), 2230.
4.	Radial Shearing Interferometer using Laser Source.	M.V.R.K. Murty and R.P. Shukla	App.Opt., Vol.12, No.11 (73), 2765.
5.	Cary Principle in Monochromator Design.	M.V.R.K. Murty	App.Opt., Vol.12, No.9 (73), 2018.
6.	Vibration-Rotation-Inversion Hamiltonian of Formaldehyde.	D.C. Moule and Ch.V.S. Ramachandra Rao.	J.Mol.Spectry., 45, 120-141 (1973).
7.	A New Electronic Transition $F^2 + - A^2$ $_1$ of AlO.	M. Singh	J.Phys.B.Atom.Mol. Phys. 6, 521 (1973).
8.	A Modified Jamin Interferometer	M.V.R.K. Murty and R.P. Shukla	Optical Engg., Vol.12, No.4, P.121, (1973).
9.	Analysis of Optical Multilayer Thin Film Filters.	K.V.S.R.Apparao	J.Opt.Soc.India (In Press).
10.	Theory of Anastigmatic Monochromator for Vacuum Ultraviolet Region.	M.V.R.K. Murty	Proc.Ind.Natl.Sci. Academy (In Press).
11.	Spectrographic Analysis of High Purity Nickel Oxide for Twenty-one Trace Impurities using a New Buffer.	N.P. Karanjikar and M.D. Saksena	Accepted for publication in Talanta.

Sl.No.	Title of the Paper	Author/s	Journal
12.	Spectrographic Analysis of High Purity Antimony for Seventeen Impurities.	P.S. Murty, S.M. Marathe, S.K. Kapoor and M. Saraswathy.	Z.Anal.Chem. 268, 285-286 (1974).
13.	Theory and Principles of Monochromators, Spectrometers and Spectrographs.	M.V.R.K. Murty	Optical Engg., Vol.13, No.1, p.23, (Jan-Feb. 1974).
14.	Spectrographic Determination of Ruthenium in Siliceous Materials.	P.S. Murty and M.J. Kamat.	Ind.J.Technology, Vol.12, No.1, p.41-42, January 1974.
15.	A Bibliography of various Testing Methods.	M.V.R.K. Murty, D. Malacara and A. Cornejo.	App.Optics (In Press).
16.	Direct Spectrographic Determination of Boron in UF_4.	P.S. Murty, S.M. Marathe and P. Rugmini Bai	Analytical Letters, 7(2), 147-151 (1974).
17.	Simultaneous Spectrographic Determination of Volatile and Refractory Impurities in Tantalum Oxide using a d.c. arc Excitation.	L.C. Chandola & Smt. V.S. Dixit	Current Science, Vol.43, No.12, 372-73 (1974).
18.	Planar Vibrations of 2-Chloropyrimidine.	Y.A. Sarma	Spectrochim. Acta (In Press).
19.	Intermittent A.C. Arc Method for the Spectrographic Analysis of Potassium Tantalofluoride.	L.C. Chandola, N.P. Karanjikar & V.S. Dixit.	Chem.Analityczna, Warsaw (In Press).
20.	Mechanism of Formation of Formaldehyde in the Flash	S.L.N.G. Krishnamacharl.	Photochemistry and Photobiology,
21.	Spectrographic Analysis of Semiconductor Grade B_2O_3.	R.V.Subramanian, R.M. Dixit and T.R. Saranathan.	Zeit.Anal.Chem. (In Press).
22.	Spectrographic Analysis of High Purity Manganese Dioxide	V.A. Job, S.B. Kartha, G.Krishnamurty & S.Gopal.	Zeit.Anal.Chem. (In Press)

BARC REPORTS PRODUCED

Sl.No.	Title of the Report	Author/s	Report No.
1.	A New Carrier for Spectrographic Determination of Silver, Molybdenum and Calcium in Uranium.	R.M. Dixit, R.V. Subramanian, P.P. Khanna and S.B. Sindgikar.	BARC-664
2.	Spectrographic Determination of Trace Impurities in Magnesium Metal.	G. Krishnamurty, Kum. Sheila Gopal and S. Krishnan	BARC-669
3.	Annual Progress Report for 1972-73.	V.B. Kartha and N.A. Narasimham	BARC-684
4.	X-ray Fluorescence Determination of Trace Impurities Nb, Fe, Mn and Ti in High Purity Ta_2O_5 and K_2TaF_7.	R.M. Agrawal and and P.P. Khanna.	BARC-698
5.	X-ray Fluorescence Analysis of Low Alloy Steels for Mo, Cu, Ni, Cr, Mn and V.	-do-	BARC-699
6.	A Normal Coordinate Analysis of Methyl Amine and its Deuterated Species.	G.S. Ghodgaonkar	BARC-700
7.	Spectrographic Analysis of High Purity Antimony for Seventeen Trace Impurities.	P. Sreeramamurty, S.M. Marathe, S.K. Kapoor and M. Saraswathy.	BARC-680
8.	Spectrographic Determination of Rare Earths Impurities in Purified Samarium Oxide.	S.V. Grampurohit & V.N.P. Kaimal	BARC-710
9.	Determination of Boron in Calcium Fluoride by Carrier Distillation Method.	S.V. Grampurohit & Smt. V.S. Dixit	BARC-714
10.	Spectrographic Analysis of High Purity Manganese Dioxide.	V.A. Job, Smt.S.B. Kartha, G.Krishnamurty and Kum. S. Gopal.	BARC-715

Sl.No.	Title of the Report	Author/s	Report No.
11.	Direct Spectrographic Determination of Boron in UF_4.	P.Sreeramamurty, S.M. Marathe and P. Rugmini Bai.	BARC-703
12.	Determination of Calcium in Uranium by X-ray Fluorescence Method.	R.M. Dixit, S.K. Kapoor and S.S. Deshpande.	BARC-729
13.	A Modified Method for the Determination of Rare Earths in High Purity Gadolinium Oxide using the Stallwood Jet.	S.V. Grampurohit & V.N.P. Kaimal	BARC-740
14.	Spectrographic Determination of Noble and other Metals in Graphite.	L.C. Chandola & Smt. V. Mahajan	BARC-738

APPENDIX IV

Break-up of Service Analysis for the year 1973

S.No.	Source	No.of samples	No.of determinations.
B.A.R.C			
1.	Analytical Chemistry Division	32	166
2.	Atomic Fuels Division	367	2513
3.	Central Workshops	2	10
4.	Chemistry Division	294	1484
5.	Chemical Engineering Division	310	1594
6.	Division of Radiological Protection	2	18
7.	Health Physics Division	5	9
8.	Heavy Water Division	37	87
9.	Isotope Division	3	18
10.	Metallurgy Division	18	110
11.	Opto-Electronics Section	1	15
12.	Reactor Engineering Division	1	7
13.	Reactor Operations Division	7	86
14.	Technical Physics Division	8	59
15.	Uranium Metal Plant	953	5078
16.	Variable Energy Cyclotron Project	3	3
Department of Atomic Energy			
17.	Atomic Minerals Division	7	72
18.	Indian Rare Earths Ltd.	7	130
19.	Power Projects Engineering Division	16	129
20.	Reactor Research Centre (FBTR Project)	12	108

S.No.	Source	No.of samples	No.of determinations
Other Institutions			
21.	Carton Chemical Industries, Bombay	10	10
22.	Century Rayon, Kalyan, Maharashtra	2	4
23.	Chemicals & Fibres India Ltd., Bombay	23	46
24.	Fertiliser Corpn.of India Ltd, Bombay	3	3
25.	Havero Industries Ltd, Bombay	11	121
26.	Indian Institute of Technology, Kanpur	1	4
27.	Indian Institute of Technology, Powai	2	38
28.	Indian Airlines	2	22
29.	Instrumentation Ltd., Kota, Rajasthan	4	18
30.	Mukand Iron and Steel Co.Ltd, Bombay	40	80
31.	Mhatre Pen & Plastic Industries, Bombay	1	1
32.	National Refineries Pvt.Ltd, Bombay	1	7
33.	Physical Research Laboratories, Ahmadabad	4	60
34.	Physics Department, D.A.V.College, Kanpur	1	4
35.	S.W.I.R.P., Pondicherry	14	70
		2204	12182